Observations of wintertime air-sea heat exchange within polynya and lead environments of Amundsen Gulf and the Southeastern Beaufort Sea

By

Christopher Stammers

A Thesis submitted to the Faculty of Graduate Studies

of The University of Manitoba

in partial fulfillment of the requirements of the degree of

MASTER OF SCIENCE

Department of Geography

University of Manitoba

Winnipeg

ABSTRACT

Direct micrometeorological measurements of heat fluxes made at the earth's surface are relatively sparse, yet the implications of these fluxes are immense on all spatial scales. Measurements are an even rarer occurrence in the Arctic, a physical environment at the forefront of scientific research. Here, we present direct measurements of wintertime surface heat fluxes between the ocean and atmosphere in lead and polynya environments in the Canadian Arctic. Environments such as those presented can yield very large vertical temperature gradients during the winter months and are particularly dynamic micrometeorological environments. We found that sensible heat fluxes can exceed +100 W m^{-2} during the winter months, much larger than most regional estimates (~ 0 W m^{-2}). In addition, large heat fluxes were shown to affect the characteristics of the near surface temperature inversion. The height, depth and strength of the characteristic wintertime inversion are shown to be influenced in cases where large surface fluxes were observed. Such findings are likely to have implications on the regional and planetary heat budget, general circulation models and larger scale weather processes, which most often omit local scale heat fluxes in their analyses and calculations.

ACKNOWLEDGEMENTS

I would like to thank my advisors, Dr. Tim Papakyriakou and Dr. David Barber for providing me with the opportunity and support throughout the course of this project. They have gone above and beyond in their guidance and patience with me on this work.

I would also like to thank colleagues Brent Else, Matthew Asplin, Rick Raddatz, Ryan Galley, Lauren Candlish, Geoff Gun, Kerri Warner and Bruce Johnson, all of whom have provided me with support in the many discussions and conversations we have had. I am also very thankful to the captains and crew of the CCGS *Amundsen* for the years of support and dedication to Arctic research. Finally, I would like to thank my committee members Dr. Jay Doering and Dr. Jens Ehn.

To my friends and family, thank you for the constant encouragement and support over the years.

DEDICATIONS

I would like to dedicate this work to my father, Kenneth Stammers, who we tragically lost in 2011.

As well, to my three friends and colleagues, Dr. Klaus Hochheim, Captain Marc Thibault and Daniel Dube, who lost their lives during the 2013 field season. Their passion and dedication to Arctic science will never be forgotten.

TABLE OF CONTENTS

LIST OF TABLES

LIST OF FIGURES

CHAPTER ONE: INTRODUCTION AND LITERATURE REVIEW

1.1 Context and Rationale

The Earth's surface has many profound effects on the atmosphere (Arya, 2001). Exchanges or fluxes between the Earth and the atmosphere, although occurring at the microscale (1 km or less), have significant effects on the Earth's meteorology and climate (Pielke et al., 1998). This coupling stems from three micrometeorological fluxes that occur at the Earth-atmosphere interface; heat (H), water vapor (E), and momentum (τ). These exchanges are driven by gradients across the air-surface interface and are facilitated by turbulent eddies of varying scales within the atmospheric boundary layer.

Ocean's cover 71 percent of the Earth's surface and are thus a crucial cover class in the global energy budget (Oke, 1987). Over typical oceans, fluxes of water vapor usually dominate over sensible heat due to small temperature differences and large moisture gradients across the air-sea interface (Oke, 1987). However, for cold, polar seas, exchanges of sensible heat are typically the dominant turbulent flux (e.g. Andreas et al., 1999). Polar seas are unique in that they experience a low solar elevation, receive little or no surface insolation during the winter, and have an annual cycle of sea ice formation and melt. It is this cycle that drives the annual cycle of insolation, resulting in large atmospheric temperature swings between seasons. Sea ice acts as an insulator between the warm ocean and cold atmosphere. The complicating factor of sea ice, with its non-uniform temporal and spatial coverage (differing age and thickness) and extreme susceptibility to changing atmospheric conditions therefore reveals a highly pertinent and critical area of research.

Sea ice remains a defining featuring of the Arctic Ocean, even under today's state of accelerated warming at high latitudes. Aside from an overall reduction in extent, sea ice cover is both thinning and undergoing a transition from multi-year to first-year ice (e.g. Maslanik, 2011; Kinnard et al., 2011; Galley et al., 2008; Comiso et al., 2008; Stroeve et al., 2005; Serreze et al., 2003; Zhang et al., 2000; Gloerson et al., 1999; Parkinson et al., 1999). The role of sea ice dynamics on heat exchange is particularly strong during the winter months, when the near surface atmosphere is at its coldest and the presence of leads (stretches of open water within fields of sea ice; Andreas et al., 1979) and polynyas (nonlinearly shaped areas of open water or new and young sea ice where thick sea ice is expected; Smith et al., 1990) within the main icepack allow for direct air-sea exchange (Smith et al., 1990; Andreas, 1999). These inhomogeneities within the icepack introduce areas where the cold Arctic atmosphere comes into contact with the relatively warm ocean. In some cases, the air-sea temperature difference in these environments may be greater than -40°C (Alam and Curry, 1997). Laikhtman and Klyuchnikova (1957) recognized that such extreme vertical temperature gradients allow for very large sensible heat fluxes. Several studies (e.g. Lupkes, 2008; Gultepe, 2003; Andreas, 1999) have shown this to be true through various parameterization schemes. Despite their limited spatial coverage (on the order of 1-5% of the total Arctic icepack) (Barry et al., 1993; Lindsay and Rothrock, 1995), open water environments contribute significantly (as high as 80%) (Marcq and Weiss, 2011) to the total ocean-atmosphere heat flux in the winter. Heat exchanges in these environments are thus are a major contributor to the wintertime planetary heat budget (e.g., Lupkes, 2008; Gultepe, 2003; Andreas, 1999; Maykut, 1978). Additionally, snowfall has increased in the Arctic (Kurtz

et al., 2011) leading to higher reflectance of solar radiation (increased depth of snowpack) but reduced heat transfer between the ocean and atmosphere (greater insulation). All of these factors have an impact on the thermodynamic and dynamic properties of sea ice and on the exchange of heat between the ocean and atmosphere (Maykut, 1982).

Although modeling studies have shown average heat fluxes over the polar seas to be less than +50 W m^{-2} (with many studies having mean H values not statistically different from 0 W m^{-2}) (Nakamura and Oort, 1988), measurements of H over smaller temporal and spatial scales, particularly in polynya and lead environments, are often much larger than regional estimates (Andreas et al., 1979; Kottmeier and Engelbart, 1991; Gultepe et al., 2003; Raddatz et al., 2011). These large heat fluxes, aside from contributing significantly to the large-scale heat budget of the Arctic (Overland, 2009), are likely to affect the temperature structure of the lower boundary layer of the atmosphere, although the extent to which is largely unknown (Lupkes, 2008; Overland and Guest, 1991; Serreze and Barry, 2005). Larger scale weather and climate processes are also likely to be affected (Simmonds and Rudeva, 2012).

By modifying the thermal structure of the lower atmosphere, linkages have been made between ocean-atmosphere heat fluxes and Arctic cyclones (eg. Simmonds and Rudeva, 2012; Asplin et al., 2012). Heat (and moisture) input from the ocean is critical in cyclone intensification and longevity (Simmonds and Keay, 2009; Higgins and Cassano, 2009), although exact linkages are not yet fully understood. As a result, cyclone frequency and intensity are increasing over the Arctic Ocean (Zhang et al, 2004). In addition, cyclones have been shown to significantly alter the icescape over a

significant area leading to greater areas of open water and enhanced heat fluxes (Asplin et al., 2012). It has been proposed that this process may help to enhance positive feedback processes that will ultimately accelerate the loss of Arctic sea ice (Asplin et al., 2012).

Ship-based measurements of surface meteorology and air-sea heat exchange were made during the 2007-08 field season as part of the International Polar Year Circumpolar Flaw Lead (IPY-CFL) study (Barber et al., 2010). The project, which ran from October through August, was the first of its kind. The CCGS *Amundsen*, a Canadian medium class icebreaker, remained mobile in Amundsen Gulf (Figure 1), allowing for the nearly continuous measurement of micrometeorological exchanges in a single region. The dataset is unparalleled in Arctic research. Throughout the study, the vessel experienced ever-changing ice conditions, including regions dominated by thin, first-year sea ice, thick multiyear ice and open water. The project's underlying goal was to "to investigate the importance of changing climate processes in the flaw lead system of the northern hemisphere on the physical, biogeochemical and biological components of the Arctic marine system" (Barber et al., 2010).

Based on previous work (e.g. Andreas et al., 1979; Maykut, 1978; Rothrock et al., 1999) air-sea heat fluxes are expected to vary significantly over time and space in response to the seasonal cycle of sea ice formation and melt, and changing atmospheric conditions. Microscale measurements of heat exchange will significantly enhance our understanding of the linkages to local environments and potentially improve our understanding of the effects of a thinning and shrinking ice cover on weather and climate over a variety of spatial and temporal scales. The objective of this work is to expand our understanding of the wintertime air-sea exchange of heat in lead and polynya

environments and evaluate their impact on the thermal structure of the lower atmosphere. The Amundsen Gulf and the Southeastern Beaufort Sea are data-sparse maritime regions of the Arctic. To our knowledge such a study is unique, and resulting insight may inform modelers on the nature of sub-grid-scale sensible heat fluxes (Andreas, 2002; Drue et al., 2007; Andreas et al., 2010a and 2010b) and air mass development within the western maritime Arctic (Penner, 1955). As the southward movement of this air mass is a significant feature of the North American climate in winter, a more realistic characterization of the thermal structure of the Arctic boundary layer may also help to improve weather simulations (Brown et al., 2006; Collins et al., 2006) below the Arctic Circle.

1.2 Thesis Objectives

The objectives of the thesis are: 1) To explore the contribution of oceanic heat exchange to the atmosphere during the 2007-08 polar winter in Amundsen Gulf and the Southeastern Beaufort Sea; 2) Identify and explain the role of surface heat transfer in affecting atmospheric boundary layer structure in dynamic mixed ice and open water environments; and 3) Investigate the representativeness of unique periods of exchange over the entire sampling period and study area.

1.3 Thesis Outline

The thesis is comprised of four additional chapters. Chapter two presents the study area where the work was conducted as well as the methods used in the data collection and analysis. Chapter three presents the results, which are then discussed in Chapter four. Chapter five concludes with a summary of our findings and a statement on future implications.

CHAPTER II: MATERIALS AND METHODOLOGY

2.1 Study Area

Measurements were made in Amundsen Gulf and the Southeastern Beaufort Sea from October 2007 through to August 2008 (Figure 1). Here, however, we focus on the wintertime component of this dataset, with unique case studies selected from January through March (Figure 1). Amundsen Gulf is located in the Canadian Northwest Territories and is the body of water constrained by Banks Island to the north, Victoria Island to the east and the continental landmass to the south. Western Amundsen Gulf is connected to the Beaufort Sea by an outlet delimited by two capes; Cape Kellett to the north and Cape Bathurst to the south. Eastern Amundsen Gulf is largely closed with the exception of small channels between Victoria Island and the North American continent.

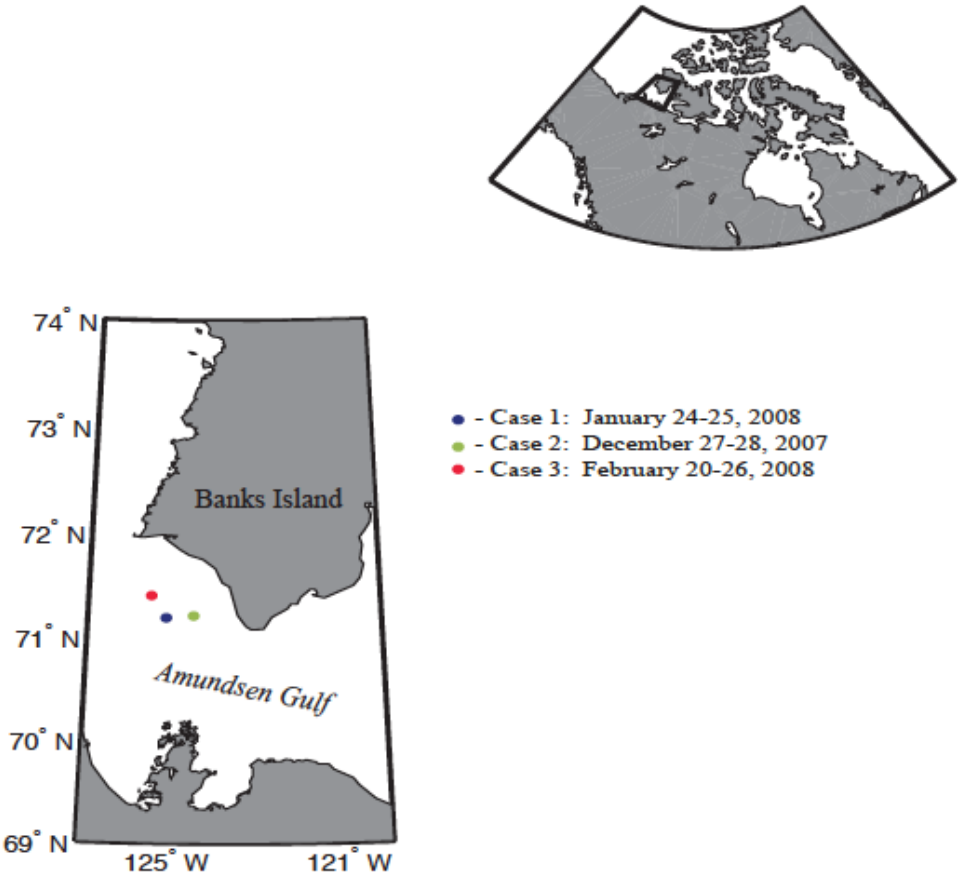

Figure 1. Study area and locations of the cases used. Points represent the midpoint of each period of study.

The meteorology of the region is Arctic marine. The effect of the annual cycle of sea ice on the large-scale meteorology of the region is perhaps best described by Overland (2009) who states that the annual cycle results in a change from a winter continental-like air mass similar to the adjacent land areas to a summertime marine air mass characterized by low cloud and fog. As a result of the annual cycle of sea ice, air temperatures during the polar winter range from between -25° to -40°C (Overland, 2009).

Cloud cover can increase surface temperatures by as much as 10°C, acting as a blanket, trapping heat near the surface (Overland, 2009).

The wintertime lower atmosphere is characterized by a stable layer that exists near the surface. This so called inversion, or region of the atmosphere where temperatures increase with height, is present daily during the winter and typically exists at heights of one to two kilometers above the surface (Bradley et al., 1992). Such inversions develop due to the presence of a cold surface layer (associated with sea ice) and result in a decoupling of the surface winds from the synoptic flow aloft (Bradley et al., 1992; Anderson and Neff, 2008). As a result, temperature inversions are much more common during winter compared to summer in the Arctic (Zhang et al., 2011).

The sea ice cycle in Amundsen Gulf is described as being characterized by extreme variability in both ice extent and thickness attributed largely to ongoing changes in the thermodynamic and dynamic forcing mechanisms (Galley et al., 2008). Freeze-up typically occurs in early October. During initial stages of ice formation, landfast ice grows along the coastal margins (Galley et al., 2008). Ice which forms offshore in Amundsen Gulf typically remains mobile during the early winter months creating an icescape that is characterized by open water environments (leads and polynyas) (Else et al., 2011). Such open water environments have a temperature near -2°C, its salinity determined freezing point (Andreas, 1999). Sea ice in the Beaufort Sea region typically remains mobile, moving with the Beaufort Gyre; a wind-driven clockwise circulating ocean current that is associated with a dominant, large-scale high pressure system in the atmosphere (Galley et al., 2008). Linear cracks or leads are also a common occurrence in this region of the Arctic (Overland et al., 1995). Polynyas, more predictable, recurring

areas of open water, are also a common feature of the regional icescape (Smith et al., 1990).

During the winter months (DJFM), the mean total sea ice coverage over the study region is 3.9 x 10^5 km^2, which represents approximately 98% coverage of the ocean surface (Galley et al., 2008). This leaves nearly 8900 km^2 (2%) of the ocean surface free of sea ice during the winter. Of the total area covered by sea ice, approximately 62% (2.5 x 10^5 km^2) is covered by first-year sea ice.

2.2 Surface Fluxes and Bulk Meteorology

We directly measure turbulent heat fluxes using the eddy covariance technique. The reader is directed to Else et al. (2011) for additional details on the ship's eddy covariance system, which are briefly described here. Eddy covariance instrumentation was mounted on a meteorological tower positioned on the foredeck near to the bow of the ship. Flux instrumentation included a sonic anemometer (Gill Windmaster Pro; installed at a height of 14 m above the sea surface or 7 m above ship deck), which was used to make high frequency measurements of the three-dimensional wind fields and sonic temperature. Basic meteorological measurements were made using a conventional anemometer (RM Young 05103; installed at a height of 15 m above sea level) for wind speed and direction, a temperature/relative humidity probe (Vasailla HMP45C212; installed at a height of 14 m above sea level) and a pressure transducer (RM Young 61205V). Data required for the motion correction was acquired using a multi-axis intertial sensing system (Systron Donner, model MotionPak) that was fixed at the

midpoint of the tower. Bulk meteorological measurements were averaged over a period of one minute. The high frequency measurements (wind, sonic temperature, humidity, angular motion) were made at 10 Hz and stored on a micrologger (Campbell Scientific, model CR3000) before being averaged over a period of 30 minutes.

Typically, estimates of the sensible heat flux (H) are calculated using some form of the bulk equation (e.g. Friehe and Schmitt, 1976):

$$H = \rho C_p C_s U \left(T_s - T_a\right) \qquad (1)$$

Where H is the sensible heat flux, ρ is the air density, C_p is the specific heat of air, U is the wind speed (typically measured at 10 meters above the sea surface), T_s is the sea surface temperature (SST), T_a is the air temperature and C_s is the sensible heat transfer coefficient (termed the Stanton number). In this method of estimating H, the air-sea temperature difference (ΔT or $T_s - T_a$) determines the direction of exchange (positive H indicates a flux towards the atmosphere or away from the surface, indicating net heat gain by the atmosphere; negative H indicates a flux away from the atmosphere or towards the surface, indicating a net heat loss by the atmosphere) while the wind velocity and transfer coefficients (along with ΔT) determine the magnitude or rate of exchange. However, transfer coefficients, such as those utilized in equation 1, are poorly understood and difficult to parameterize in time and space (e.g. Chou, 1993; Blanc, 1985; Grachev and Panin, 1984; Kondo, 1975), even more so for the world's high latitude seas where sea ice, amongst other phenomena, becomes a complicating factor. For these reasons, the eddy covariance technique becomes a much more intriguing and appropriate method for calculating surface fluxes (see Baldocchi, 2003; Twine, 2000; Webb, 1980 or Goulden, 1996).

Measurements of wind and temperature are typically made between 10-20 Hz by the sonic anemometer. The vertical flux of heat is defined as the covariance of the vertical wind velocity and the sonic air temperature. It is defined by the following equation:

$$H = \rho_a C_p \overline{w'T'} \qquad (2)$$

where H is the sensible heat flux (W m^{-2}), ρ_a is the air density (kg m^{-3}), C_p is the specific heat of air (J kg^{-1} K^{-1}), w is the vertical wind velocity (m s^{-1}) and T is the sonic temperature (K). Note that the prime symbol denotes an instantaneous fluctuation and the overbar denotes a time average.

Details on the application of the technique are available in Else et al. (2011). In brief, high frequency temperature measurements were derived from the sonic temperature following (Kaimal and Gaynor, 1991). Motion correction was applied to *w* following Anctil et al. (1994), using the 3-axis measurement of acceleration and angular velocity from the MotionPak sensor. Fluxes were computed over a 30-minute averaging period. Flux intervals were rejected if within each averaging period there were significant changes in any of speed over ground, heading or course over ground. The flux period was rejected if ship speed (for periods where the ship was under power) deviated by ±3.7 km hr^{-1} from the mean and if ship course deviated by ±27.5° from the mean. Wind direction was required to be within ±27.5° of the mean and restricted to within ±90° of the bow of the ship. The mobile nature of the system allowed for the measurement of unique environments that would otherwise be inaccessible. Our main challenge was that sensors were subject to freezing spray and icing (Else et al., 2011). Extensive filtering was required to remove those periods when atmospheric conditions significantly affected the

meteorological instruments. Overall there were 3841 usable flux-averaging intervals after screening of biased data. We opted to break the time series into case studies to examine heat fluxes within non-homogenous surfaces.

2.3 Sea Ice

Sea ice conditions were assessed using RADARSAT-1 imagery for each individual case study. Specifically, ScanSAR narrow beam images were used. These images have a resolution of 50 m and cover an area of 90,000 km^2 (300 x 300 km). Images were classified by ice type and thickness and obtained for the appropriate dates used in the analysis. Images represent approximately the mid-point of the period of time for each case study. Sea ice concentration, open water and ice type were determined for each of the case studies analyzed using methods outlined by Galley et al., (2008).

Sea ice conditions for the entire study period were analyzed using AMSR-E imagery. Weekly, 1000 kilometer resolution (or less) images were obtained for each flux averaging period and, given the ship's position, were classified as being 1) no open water, all relative to the ship's position, 2) near open water (at a minimum distance of 10 meters and a maximum distance of 1 kilometer upwind), and 3) in open water. This allowed for an estimate of how often during the study the ship experienced significant open water conditions (defined as 7/10ths or less sea ice coverage). Finally, mean fluxes were computed for each of the three categories used in the classification.

2.4 Atmospheric Temperature Profiles

Atmospheric profiles of temperature and humidity were collected over the course of the study using a microwave radiometric profiler (MWRP) that was situated behind the bridge of the research icebreaker *Amundsen* (see Candlish et al., 2012). Profiles were measured to a vertical height of 10 kilometers above the surface. The profiler provides high temporal resolution profiles of temperature (K), absolute humidity (g m^{-3}) and liquid water (g m^{-3}) every minute. The Radiometrics MP-3000A profiler had been previously validated against radiosonde profiles (Candlish et al., 2012). Temperature profiles in the lowest two kilometers were shown to exhibit differences of less than 2 K for the winter season, the smallest differences of the four seasons. Additional information on our deployment of the profiler is available in Candlish et al. (2012) and Raddatz et al. (2013).

Vertical temperature profiles were constrained to the lowest two kilometers of the atmosphere for this particular study. This represents the layer of the atmosphere that is most significantly affected by surface exchanges and interactions. This turbulent layer of the atmosphere is often referred to as the planetary boundary layer (PBL or BL) and typically extends to an average height of one kilometer in the Arctic (Raddatz et al., 2013; Overland, 2009). Ten-minute averages of the MWRP vertical profiles were computed to correspond closely with the averaging period used in calculating surface fluxes.

As mentioned, temperature inversions are a dominant feature over sea ice in the Arctic winter (Overland, 2009; Curry et al., 1996). They represent a stable region of the atmosphere that inhibit upward movement of rising air parcels (thermals) and are a

dominant feature of the vertical temperature structure of the Arctic boundary layer (Raddatz et al., 2012). Because of their importance and regularity in the Arctic, inversion characteristics were deemed to be an appropriate means of analysis in studying the role of high surface exchanges in modifying the temperature profile of the lower atmosphere during the polar winter.

Three characteristics of near surface inversions were determined and used in the analysis: 1) height, 2) strength, and 3) depth. Inversion height is defined as the height in the atmosphere where temperatures begin to increase with height. Inversion strength is defined as the temperature difference in the inversion (difference between the warmest and coldest temperatures in the layer of increasing temperatures). Finally inversion depth is defined as the thickness over which temperatures increase (height difference between where temperatures begin to increase and subsequently begin to decrease again with height). For this study, we adopt the definition of temperature inversion used by Kahl (1990) and Serreze et al. (1992), which includes thin (<100 m) embedded layers where temperature decreases with height within the main layer of increasing temperature.

CHAPTER III: RESULTS

The wintertime mean surface heat flux was -0.016 W m^{-2} (small heat loss by the atmosphere) and was shown to be not significantly different from 0 (p-value of 0.952). This mean value is confirmed by literature such as Overland (2009) and Sirevaag et al. (2011) who found similar averages over sea ice in the winter. The mean sensible heat flux for January was +0.712 W m^{-2}, +0.524 W m^{-2} for February and -1.48 W m^{-2} in March. The small mean heat fluxes presented here are typical of wintertime marine environments where sea ice dominates the surface (Raddatz et al., 2013).

Figure 2 highlights the range of values observed throughout the ship track. The distribution of H shown in Figure 2 is presented in Figure 3. Note that the vast majority (roughly 94 percent) of heat flux values range from between -50 and +50 W m^{-2} with very few exceeding 100 W m^{-2} (roughly 4 percent). Also notice that, in support of the overall mean H, the distribution slightly favors negative heat fluxes.

Details on the relationship between the measured fluxes and sea ice microenvironment are described in the following section. H values in some of these unique environments are shown to be as high as +100 W m^{-2}, much larger than regional estimates used in climate models. Three cases were selected for analysis (Table 1). Cases were selected on the basis of ice environment (unique open water, lead or polynya feature) or observed fluxes (greater than +100 W m^{-2} or statistically different from the mean).

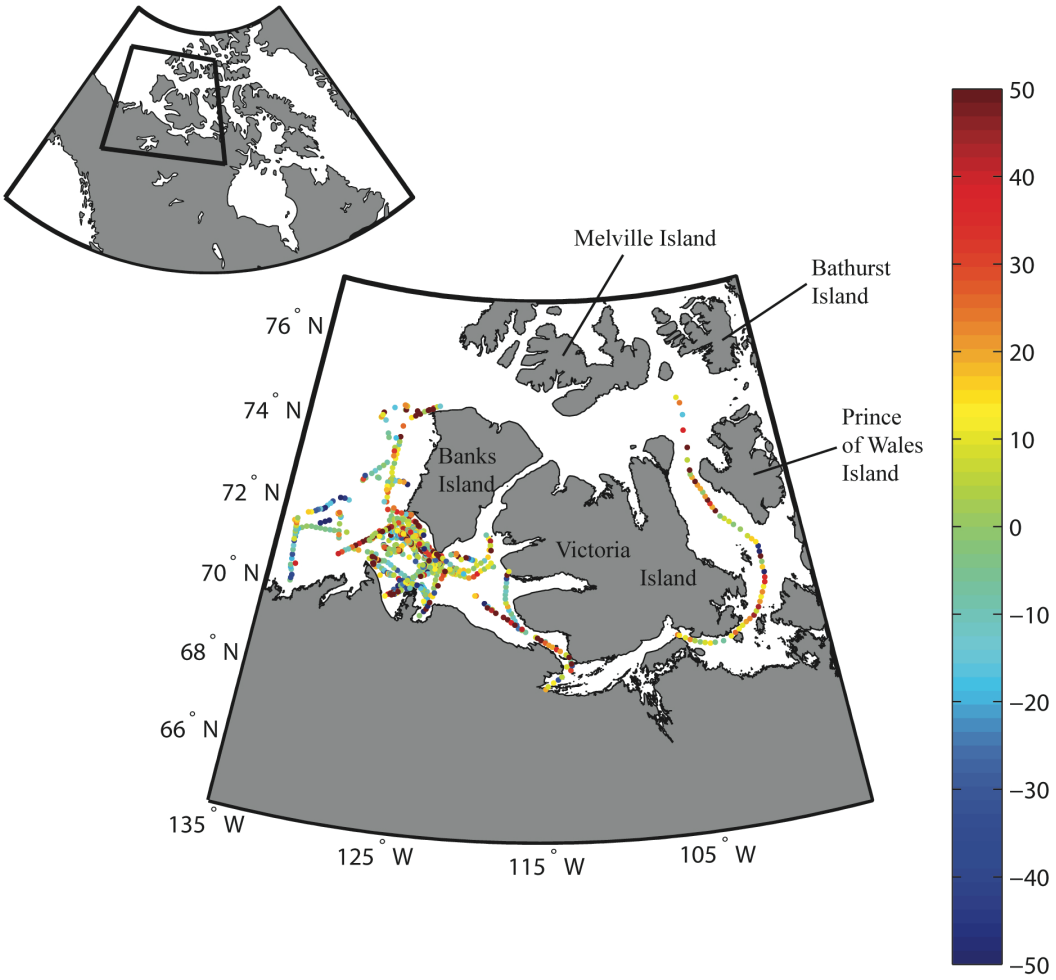

Figure 2. Calculated air-sea sensible heat fluxes during the 2007-2008 CFL field study, following the ship track of the CCGS Amundsen. Heat fluxes are shown in W m^{-2}.

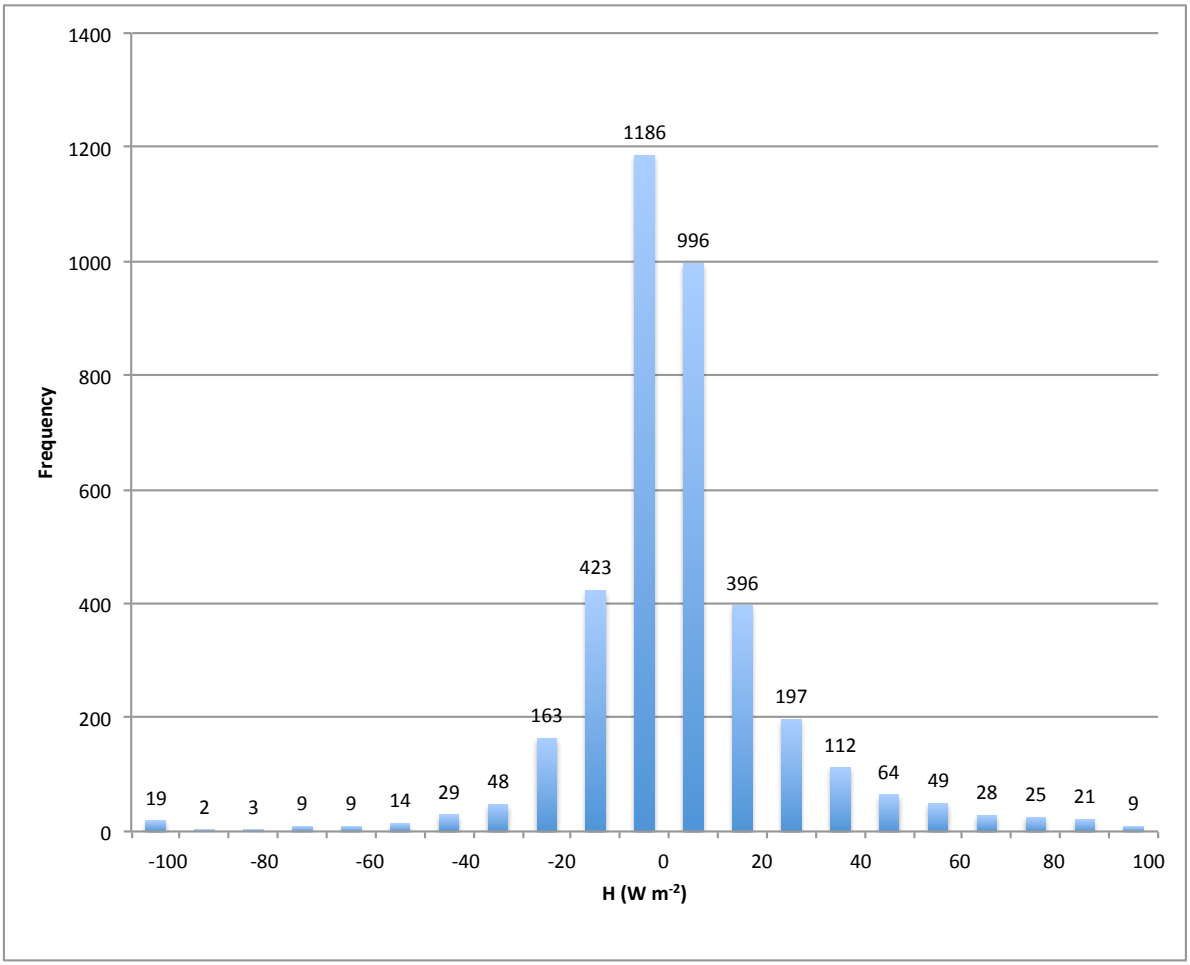

Figure 3. Frequency distribution of H (W m^{-2}) over the entire sampling period (3841 flux averaging intervals).

Case Number	Date	Latitude (°)	Longitude (°)	H flux (W m^{-2})	Air T (°C)	Wind Velocity (m s^{-1})	Wind Direction (°)
1	January 24-25, 2008	71.19	-125.1	10.0	-21.6	8.9	259.9
2	December 27-28, 2007	71.21	-124.48	1.9	-21.9	5.4	122.2
3	February 20-26, 2008	71.40	-125.49	16.0	-15.3	8.5	134.4

Table 1. Summary of the cases used. Latitudes and longitudes shown are the midpoints of the ship's position during the time period. H, T and wind variables are the mean value during the time period.

3.1 Surface fluxes

3.1.1 Case 1: January 24-26, 2008; Young sea ice and lead networks

Flux measurements were made from January 24-26, 2008 (figures 4 and 5). During this part of the cruise the vessel experienced large, positive heat fluxes on the order of +95 W m^{-2}; much larger than expected in a winter Arctic icescape dominated by multiyear and thick first-year sea ice. The mean sensible heat flux for this period was +10 W m^{-2}, also significantly higher than typically reported wintertime values.

Analysis of the ice environment where the ship was positioned revealed small pans of older first-year ice (70-120 cm thick) interspersed amongst younger first-year ice (< 30 cm thick). Small lead networks and open water environments were also present in this newly formed ice.

Mean air temperature during this period was -21.6°C. Surface temperatures where regions of open water were present were slightly warmer than -2°C, the freezing point of seawater. This meant that air-sea temperature differences were on the order of 20°C. Wind speeds were also considerably high during the period (mean of 8.9 m s^{-1}), especially during the times when enhanced surface exchanges were observed (mean direction of 260° or westerly relative to the ship). A peak wind speed of roughly 18 m s^{-1} was observed around 17:00, which corresponded to the largest observed heat flux of roughly +95 W m^{-2}. Air temperatures, however, were at their coldest later in the period.

These features, along with strong winds (on the order of 18 m s^{-1}), combined to produce the large air-sea heat fluxes observed between 15:00 and 21:00 on January 24.

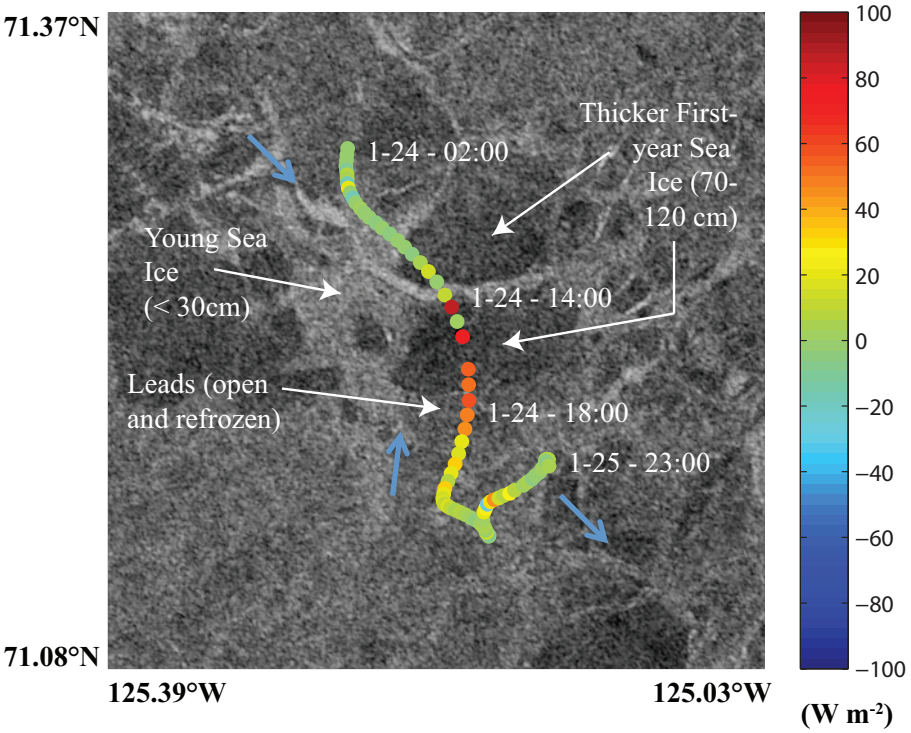

Figure 4. Spatial and temporal variation of H for Case 1. Wind direction at various points along the ship track are shown by the blue arrows.

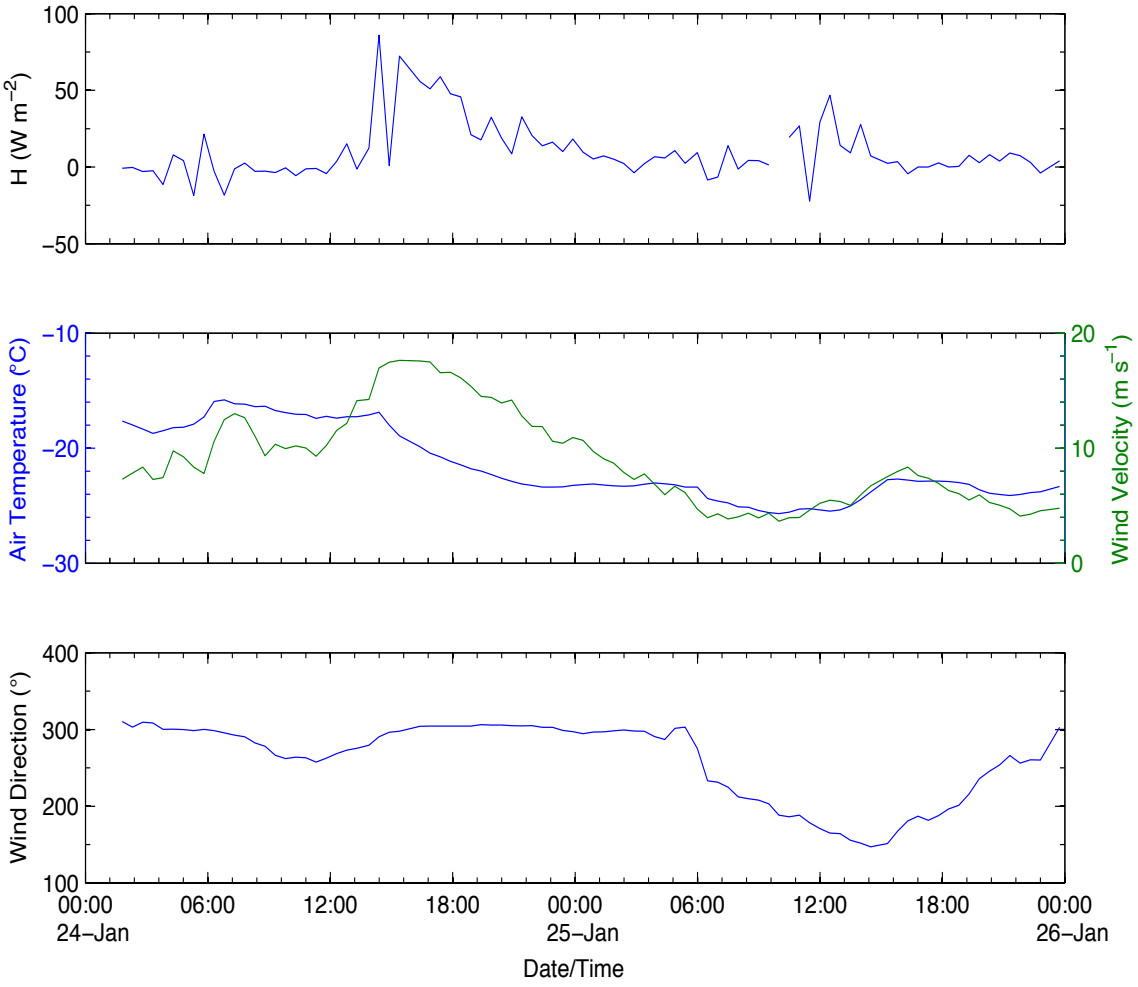

Figure 5. Times series of H, air temperature, wind velocity and wind direction for Case 1.

3.1.2 Case 2: December 27-28, 2007; Uniform icescape dominated by first-year sea ice

Flux measurements were made from December 27-28, 2007 (figures 6 and 7). During this part of the cruise, the vessel experienced relatively uniform ice conditions, composed mostly of young, first-year sea ice. Sensible heat fluxes measured were fairly uniform over this period (average of roughly 2 W m^{-2}) compared to case 1 where the sea ice conditions were much more variable (resulting in a much larger mean H). Heat fluxes over this period consistently ranged from between -20 and +20 W m^{-2} (small heat gains and losses by the surface).

Sea ice conditions experienced by the CCGS *Amundsen* during this period of study were much more uniform than cases 1 and 3. Sea ice in the region consisted of young, first-year sea ice on the order of 30 cm thick or less. Very little open water (<15%) is present in the image used for this period. A large lead in the eastern portion of the image was responsible for the majority of the open water fraction estimated. However, the low sensible heat fluxes measured suggest that the ship was not influenced by the presence of this lead.

Wind speeds also remained much lighter over the period (<8 m s^{-1} until late in the period) compared to case 1. This likely did not promote as much turbulent mixing, which ultimately aids in sensible heat transfer. With the exception of a shift in wind direction from more northerly to southerly early in the period, wind direction also remained fairly consistent. The combination of consistent wind variables, much lighter wind speeds (compared to case 1) and uniform sea ice coverage with little open water resulted in

uniform and relatively small heat fluxes away from and towards the surface during this period of study.

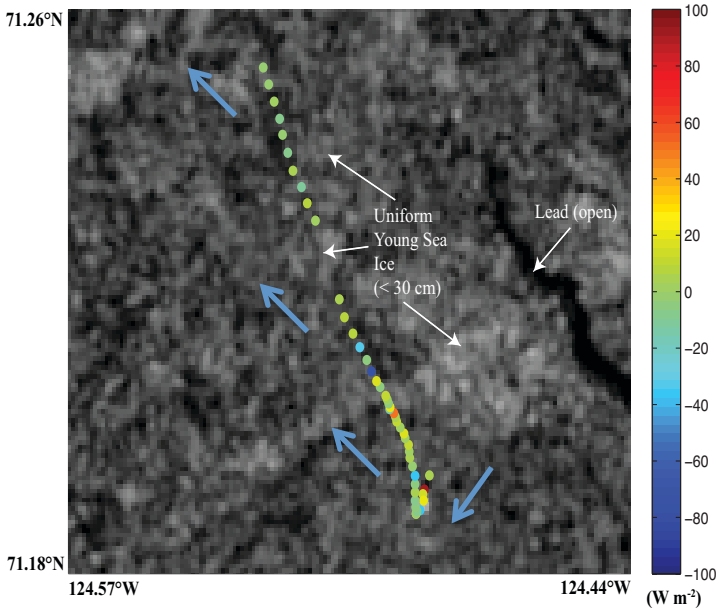

Figure 6. Spatial and temporal variation of H for Case 2. Wind direction at various points along the ship track are shown by the blue arrows.

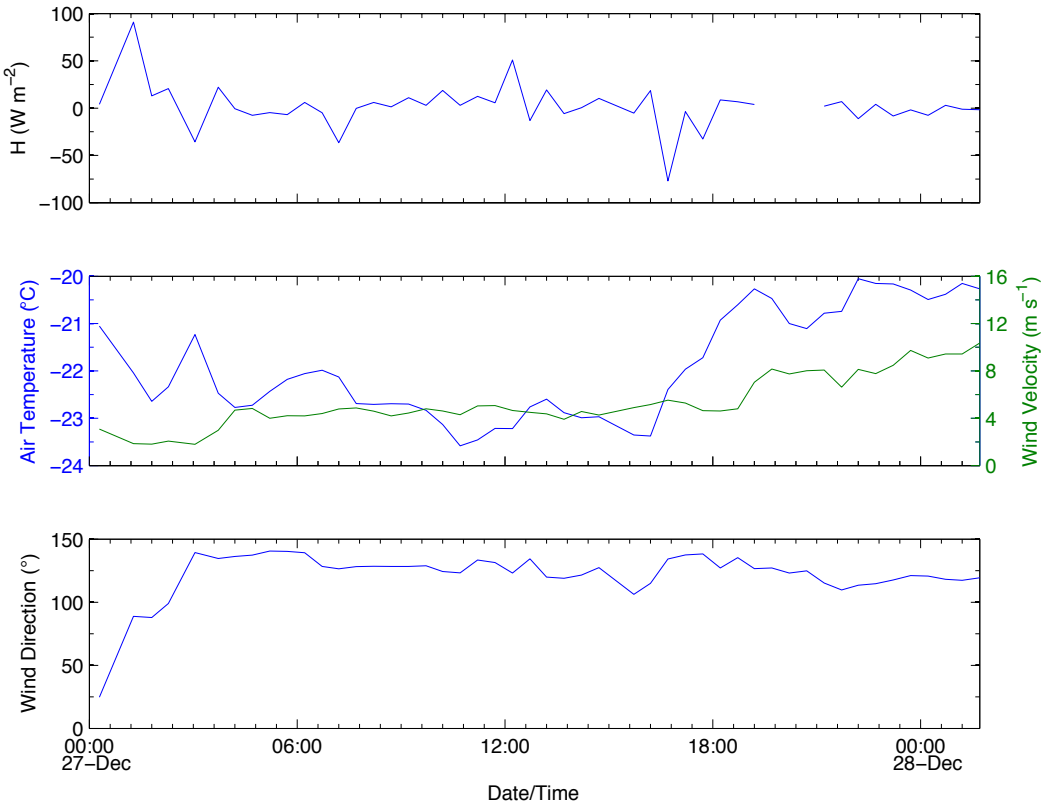

Figure 7. Times series of H, air temperature, wind velocity and wind direction for Case 2.

3.1.3 Case 3: February 22-24, 2008; Open leads

Flux measurements were made from February 22-24, 2008 (figures 8 and 9). During this part of the cruise, vessel was subject to a dynamic icescape characterized by many frozen and unfrozen leads interspersed amongst areas of older, first year ice. In these open water environments, heat fluxes as high as +105 W m^{-2} were measured (mean of 16 W m^{-2}), comparable with those observed in case 1. In areas where thicker, first-year ice was present (especially later on in the period), much smaller heat fluxes were measured, as would be expected. To the contrary, heat fluxes were quite large and positive in environments of open water and newly frozen sea ice.

Sea ice conditions were much more variable in case 3. The icescape consisted of several areas of open and newly frozen leads (as compared to one main area of open water in case 1 and no open water in case 2) as well as pans of thin to medium thickness first-year sea ice (70-120 cm). Large, positive sensible heat fluxes were observed in leads that were either open or refrozen. Much smaller heat fluxes were observed in the thicker ice that the ship encountered earlier and later in the period.

The average air-sea sensible heat flux for this period was approximately +16 W m^{-2}, nearly double the average of case 1. Although wind speeds were less variable for this period (albeit only slightly compared to case 1), the larger open water coverage was likely the reason for the enhanced exchange measured. As wind speeds diminished slightly late in the period, sensible head fluxes decreased likewise. Air temperature remained fairly uniform around -15°C, dropping only slightly later in the period.

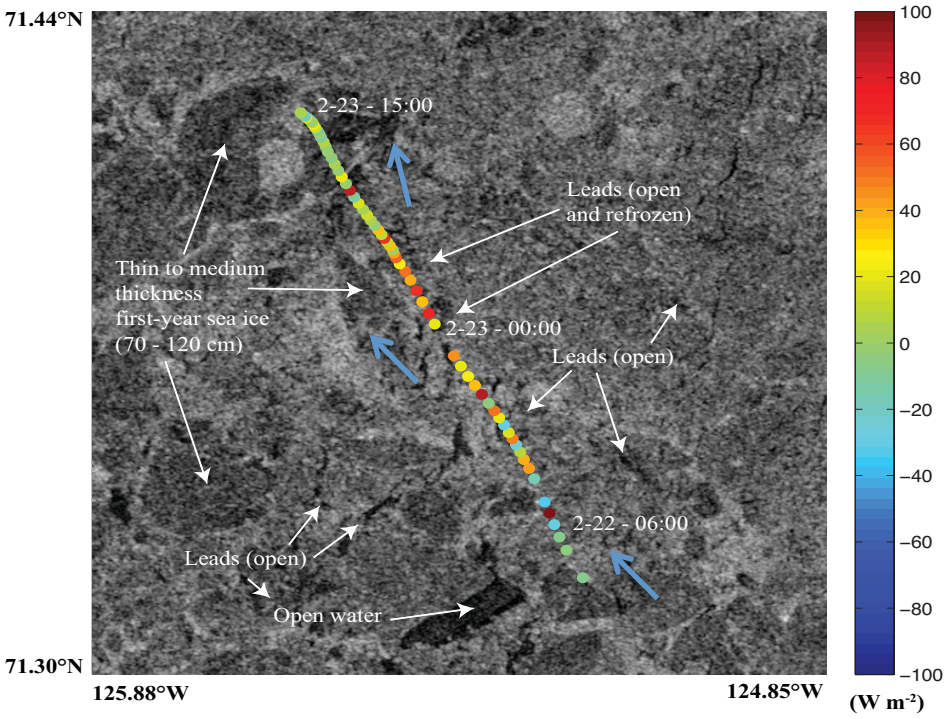

Figure 8. Spatial and temporal variation of H for Case 3. Wind direction at various points along the ship track are shown by the blue arrows.

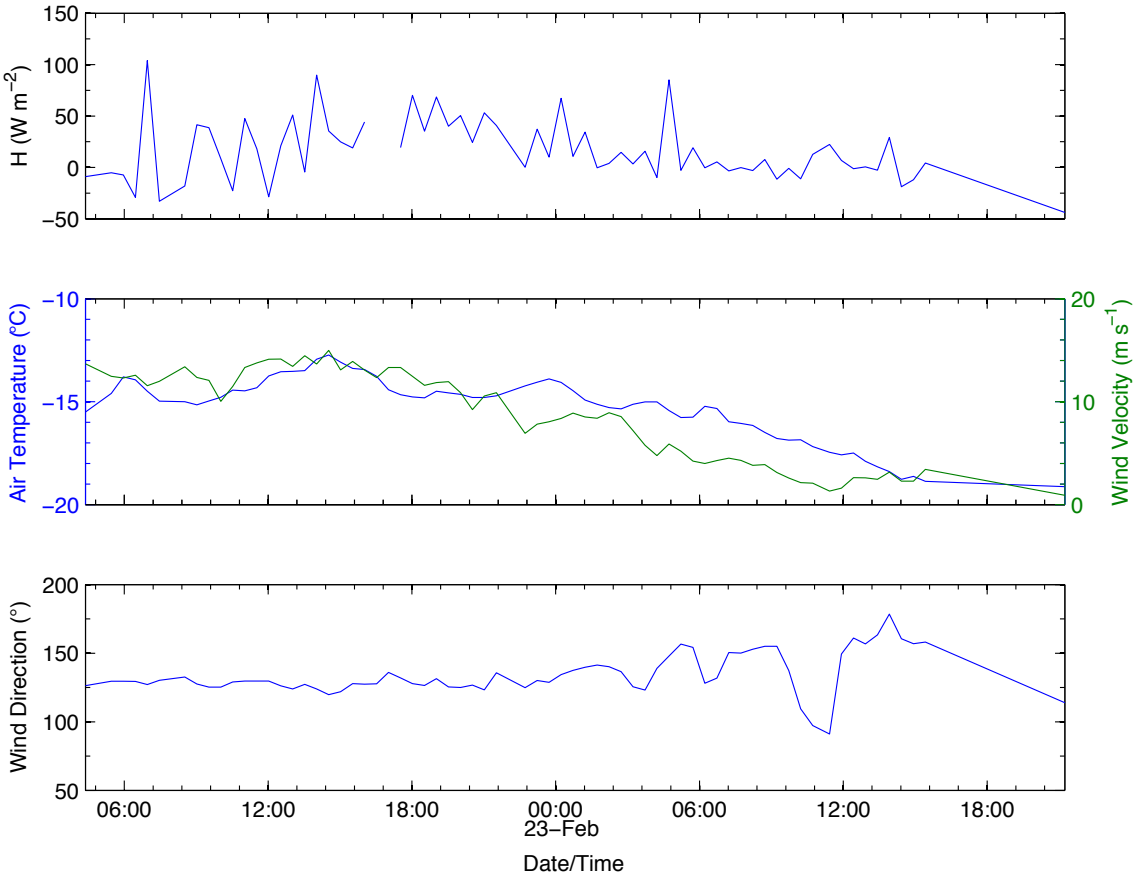

Figure 9. Times series of H, air temperature, wind velocity and wind direction for Case 3.

3.2 Effects on the boundary layer

Linkages between surface characteristics, meteorology and the air-sea exchange of sensible heat, while important, do not uncover the role that such exchanges play in affecting the atmosphere. In particular, periods of intense surface exchange can modify the characteristics of the near surface temperature inversion, a defining feature of the atmospheric boundary layer over the Arctic Ocean during the winter. Overall, inversions were found to be present in roughly 91% of cases analyzed for this study. This is comparable to Raddatz et al. (2011) value of 97% for wintertime cases. Here, we uncover one such example where exchanges of heat from the ocean are shown to affect the temperature structure (or profile) of the lower atmosphere (herein referred to as the atmospheric boundary layer or BL), as measured by a microwave radiometric profiler.

Case 1 provides an ideal framework for a study of this nature. Recall that this case involved transiting through young and newly frozen lead networks. Large heat fluxes on the order of +95 W m^{-2} were measured in open water environments during the period. Recall also that the period of enhanced exchange (herein identified as a measured flux of 2.5 times the mean or greater) occurred between 15:00 and 21:00 on January 24, 2008. Positive fluxes such as this indicate warming of the atmosphere. For this case study, mean inversion height, strength and depth were calculated over the duration of the period. In addition, three soundings were extracted from the time series; one prior, during and after the period of enhanced exchange that occurred between 15:00 and 21:00 on January 24. The times of the chosen soundings are shown in Table 2.

	Inversion Height (km)	Inversion Strength (K)	Inversion Depth (km)
2008-01-24 10:00	0.6	0.75	0.3
2008-01-24 18:00	0.45	0.25	0.55
2008-01-25 05:00	0.6	0.45	0.3

Table 2. Summary of inversion characteristics prior, during and after the period of enhanced exchange that occurred between 15:00 and 21:00 on January 24.

3.2.1 Inversion height

The first parameter of interest is inversion height (Figure 10). Mean inversion height for the period was found to be 0.39 km. This is considerably lower than Curry et al.'s (1996) estimate of mean wintertime inversion height over the Arctic Ocean. They estimated that mean inversion height ranged from 0.5 to 1.5 km over sea ice during the winter. Similar heights to Curry et al. (1996) were found by Serreze et al. (1992).

Consider the case 1 time series of H and inversion height. Inversion height ranges from 0 (no inversion) to 0.8 km. During periods of enhanced surface exchanges (greater than +25 W m^{-2} or 2.5 times the mean), such as between 15:00 and 21:00 on January 24, the height of the near surface inversion is shown to decrease (highlighted by the red bounding box). In other words, enhanced surface exchanges of sensible heat can contribute to the evolution of the lower boundary layer temperature profile such that the height of the wintertime inversion is lowered. The same was observed for other periods of enhanced heating of the lower boundary layer.

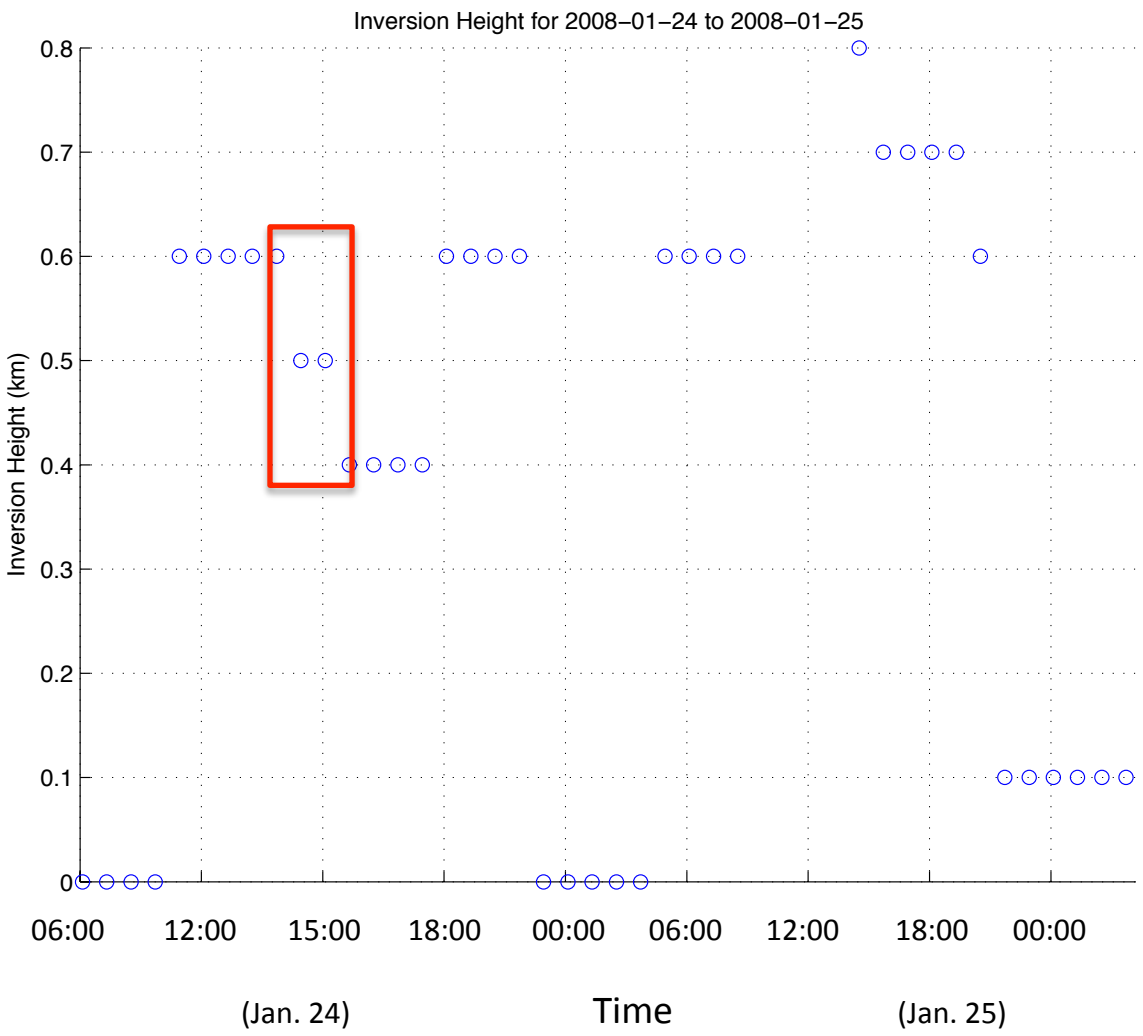

Figure 10. Time series of inversion height for Case 1.

3.2.2 Inversion strength

Inversion strength is the second parameter of interest (Figure 11). Mean inversion strength for the period was found to be 0.30 K. This is significantly smaller than values found by a similar analysis conducted by Pavelsky et al. (2010). The study estimated inversion strength over sea ice using AIRS, NCEP and ERA-40 reanalysis data and found the mean wintertime inversion strength to be between 1.53 and 2.80 K (depending on the product used). The mean wintertime inversion strength found by Pavelsky et al. (2010) is roughly 1 to 2 K stronger than our study. While Pavelsky et al. considered the entire Arctic Ocean, this study considers only a highly localized environment so it is expected that mean values will differ significantly.

Consider the case 1 time series of H and inversion strength where inversion strength varies from 0 (no inversion present) to 3 K. During periods of enhanced surface fluxes (greater than +25 W m^{-2}) such as between 15:00 and 21:00 on January 24, inversion strength was notably weaker. Since these fluxes were largely attributed to open water and thin ice, the results follow suit to that of Pavelsky et al (2010), namely that wintertime inversion strength is strongly dependent on the sea ice concentration. Inversion strength was found to increase with increasing sea ice concentration ($r = 0.78$).

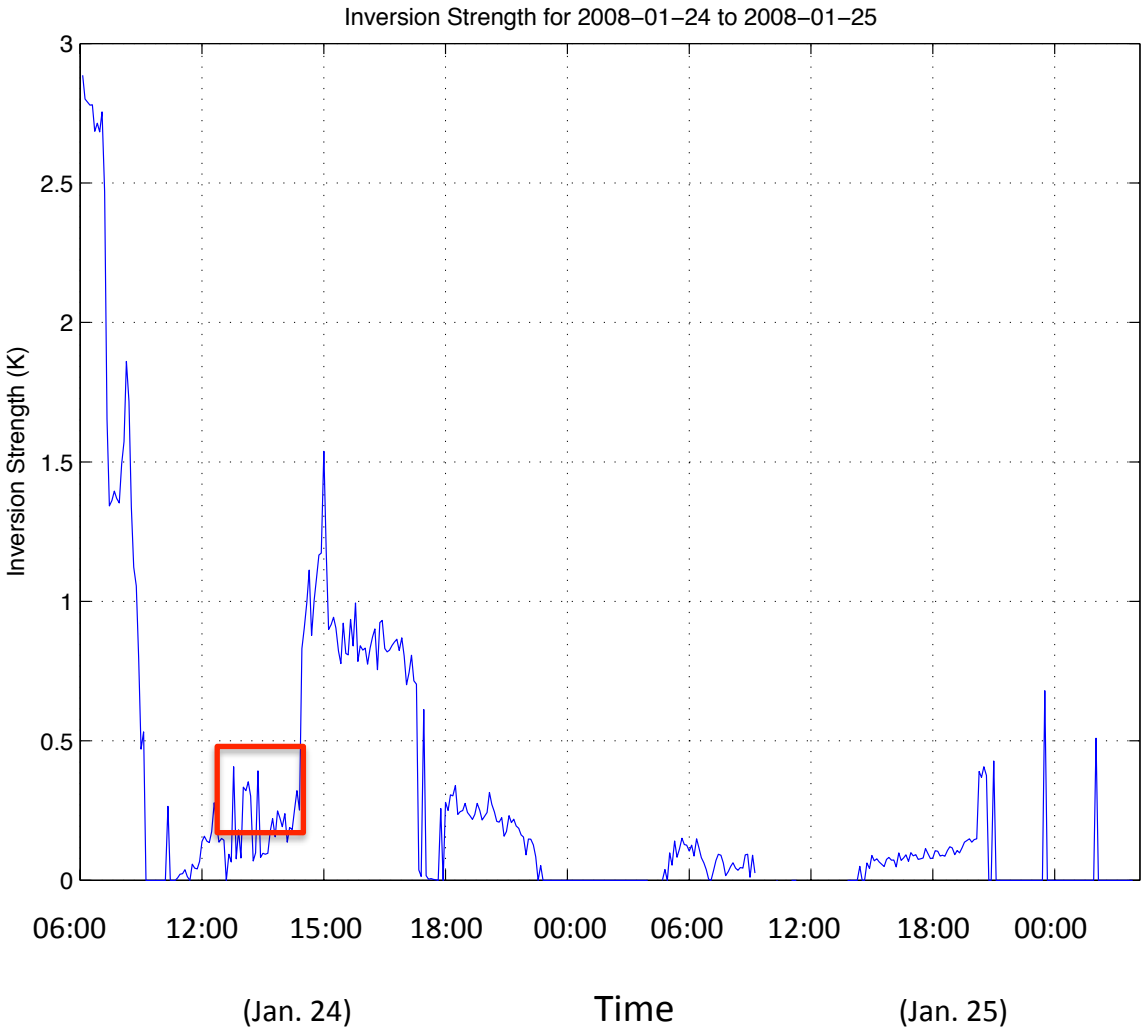

Figure 11. Time series of inversion strength for Case 1.

3.2.3 Inversion depth

Inversion depth is the final parameter of interest (Figure 12). Mean inversion depth for the period was found to be 0.24 km. Kahl (1990) found that mean inversion depth ranged from 0.25 to 0.80 km over the course of sea ice freeze-up (fall) and maximum ice coverage (late winter). Our wintertime mean inversion depth of 0.24 km seems reasonable given that it is only slightly smaller than the range of values found by Kahl (1990).

Consider the case 1 time series of H and inversion depth where inversion depth ranges from 0.05 to 0.6 km. During periods of enhanced surface fluxes (greater than +25 W m^{-2}) such as between 15:00 and 21:00 on January 24, inversion depth has been shown to increase (such as from 0.3 to 0.6 km over the mentioned period). In other words, inversions become deeper when strong heat fluxes from the surface modify the atmospheric column. This is due to warming of the lower layers of the atmosphere.

Further to analyzing inversion height, strength and depth, three vertical temperature profiles were extracted for this case study: one prior (10:00), one during (18:00) and one after (05:00 on the 25th) the period of enhanced exchange observed between 15:00 and 21:00 on January 24 (Table 2). From the values in Table 2, we can see that the same observations for inversion strength follow suit. The height of the inversion is lower during the period of higher sensible heat exchange (0.45 km down from 0.6 km). Inversion strength is also reduced for the sounding extracted during the period of highest surface fluxes (0.25 K) and responds afterwards. Finally, inversion

depth increases (0.55 km up from 0.3 km) during the period of enhanced exchange. This further illustrates the response of the boundary layer inversion during periods of enhanced surface fluxes as well as the temporal scale of the response prior, during and after such an event.

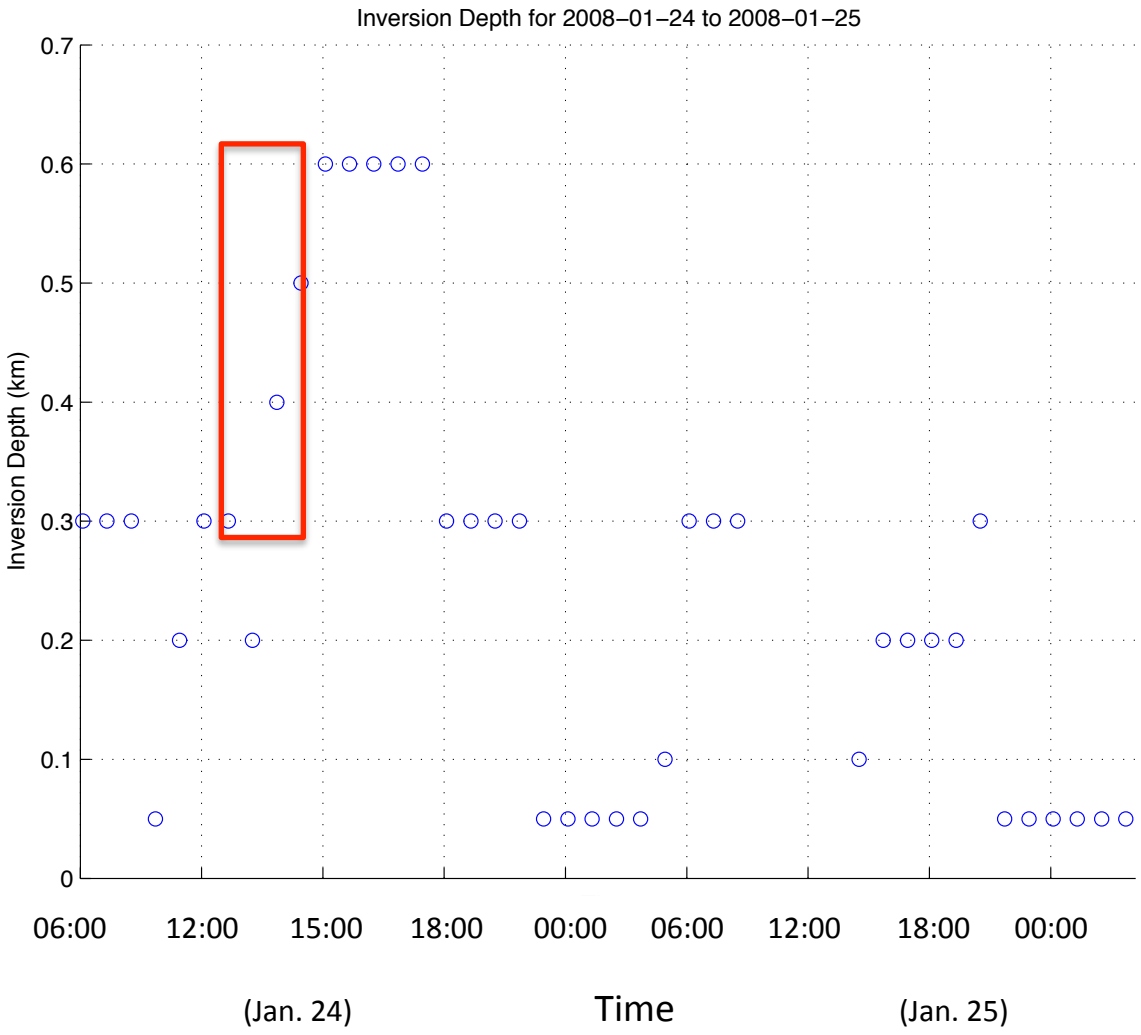

Figure 12. Time series of inversion depth for Case 1.

3.3 Representativeness of cases

We have presented three cases where large sensible heat fluxes were measured in open water environments (less than 7/10ths sea ice coverage) and here I comment on the representativeness of these cases over the span of the entire study. We classified the ship's position, using AMSR-E ice images for each flux averaging interval, as being in open water, near open water or no open water nearby. We found that, of the 3841 flux averaging intervals, the ship experienced no open water (7/10ths or greater ice coverage) 70 percent of the time (or 2713 intervals). The ship was therefore influenced by open water (7/10ths or less sea ice coverage) 30 percent of the time (or 1128 intervals). Specifically, the ship was near open water (less than 1 km upwind) around 27 percent of the time (or 1021 intervals) and in open water 3 percent of the time (or 107 intervals). Literature such as Pinto et al., 2003 estimated a flux footprint of 2.5 km so our threshold of 1 km is appropriate. The distribution of the different categories is shown in Figure 13.

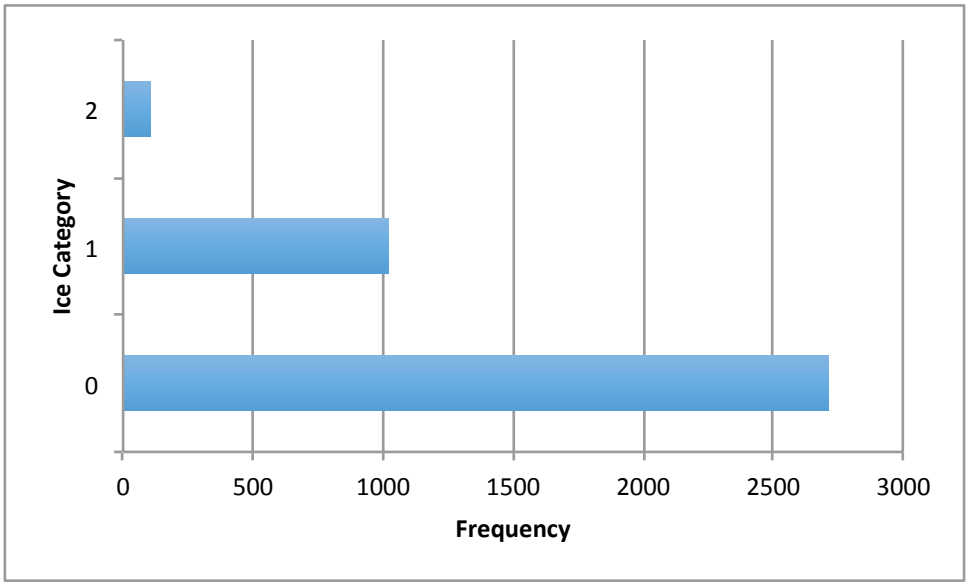

Figure 13. Distribution of the 3841 flux averaging periods for the three different ice classification regimes (0 – No open water; 1 – Near open water; 2 – In open water).

Mean fluxes were also computed for the three different classification regimes. Cases where there was no open water had a mean sensible heat flux of 2.1 W m^{-2}. Cases where the ship was near open water had a mean flux of 6.4 W m^{-2} while cases that were in open water had a mean flux of 2.9 W m^{-2}. Note that when the ship was being influenced by open water fluxes were higher than when there was no open water. In the cases where the ship was upwind of open water features, fluxes were considerably higher. Figures 14 through 16 present the distribution of heat fluxes for the three different ice classification regimes. The quartiles for each histogram are summarized in table 3.

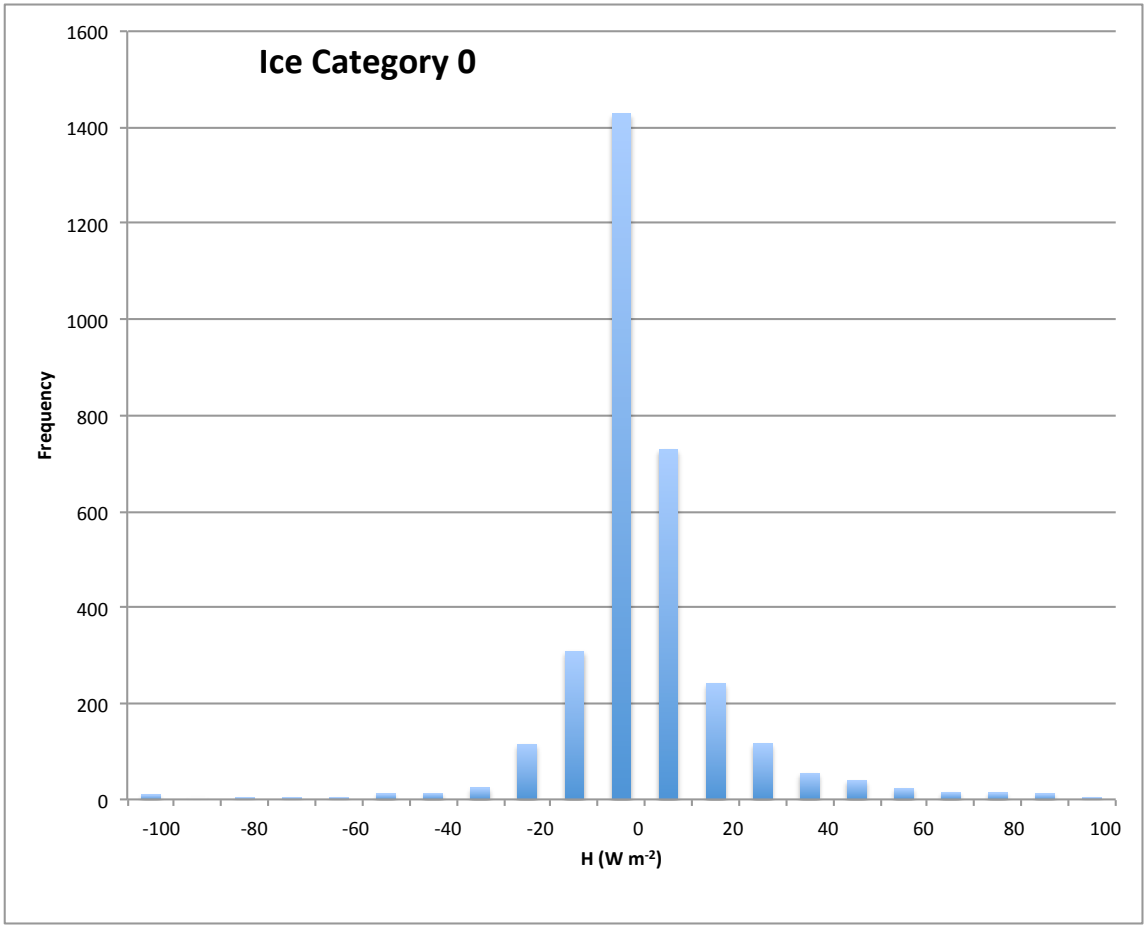

Figure 14. Distribution of sensible heat flux for ice category 0 – no open water (7/10ths or more sea ice).

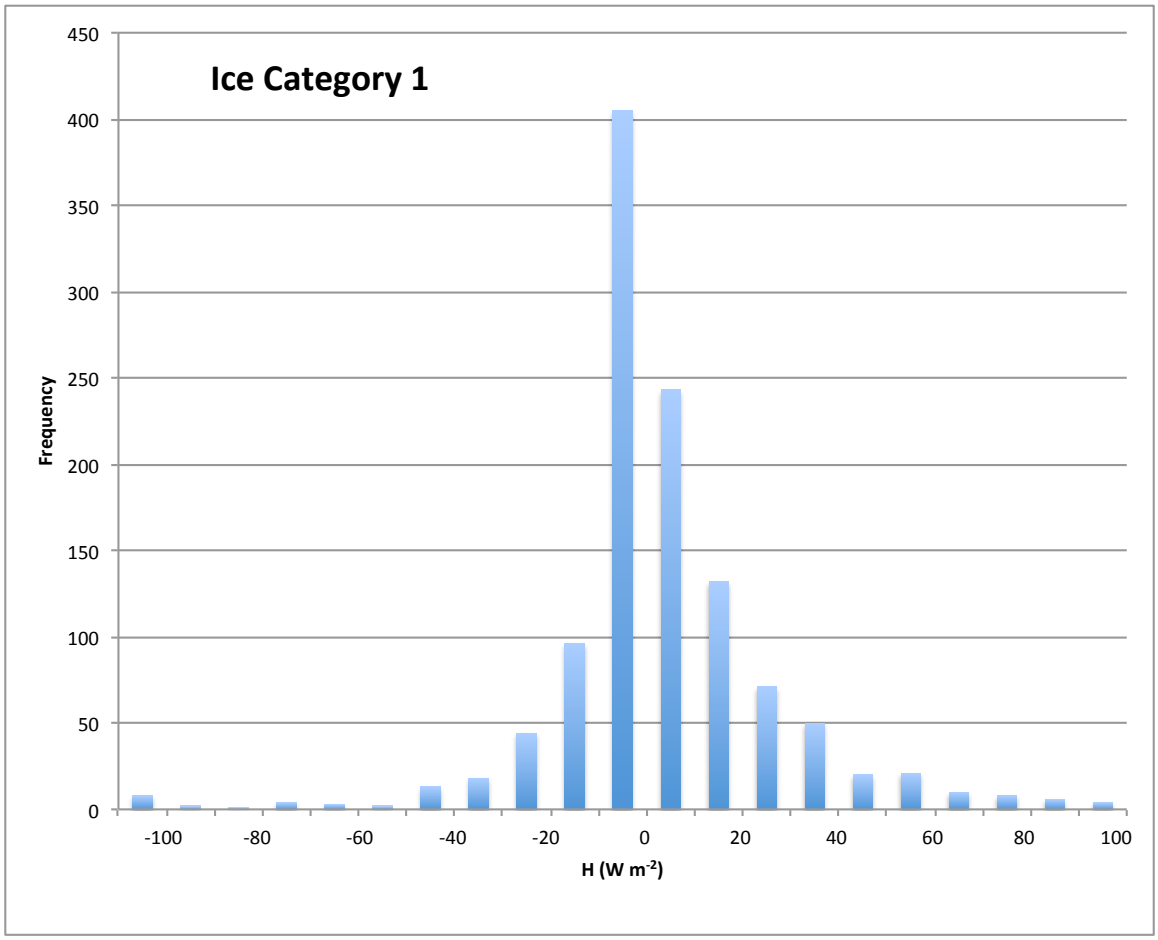

Figure 15. Distribution of sensible heat flux for ice category 1 – near open water (less than 7/10ths sea ice).

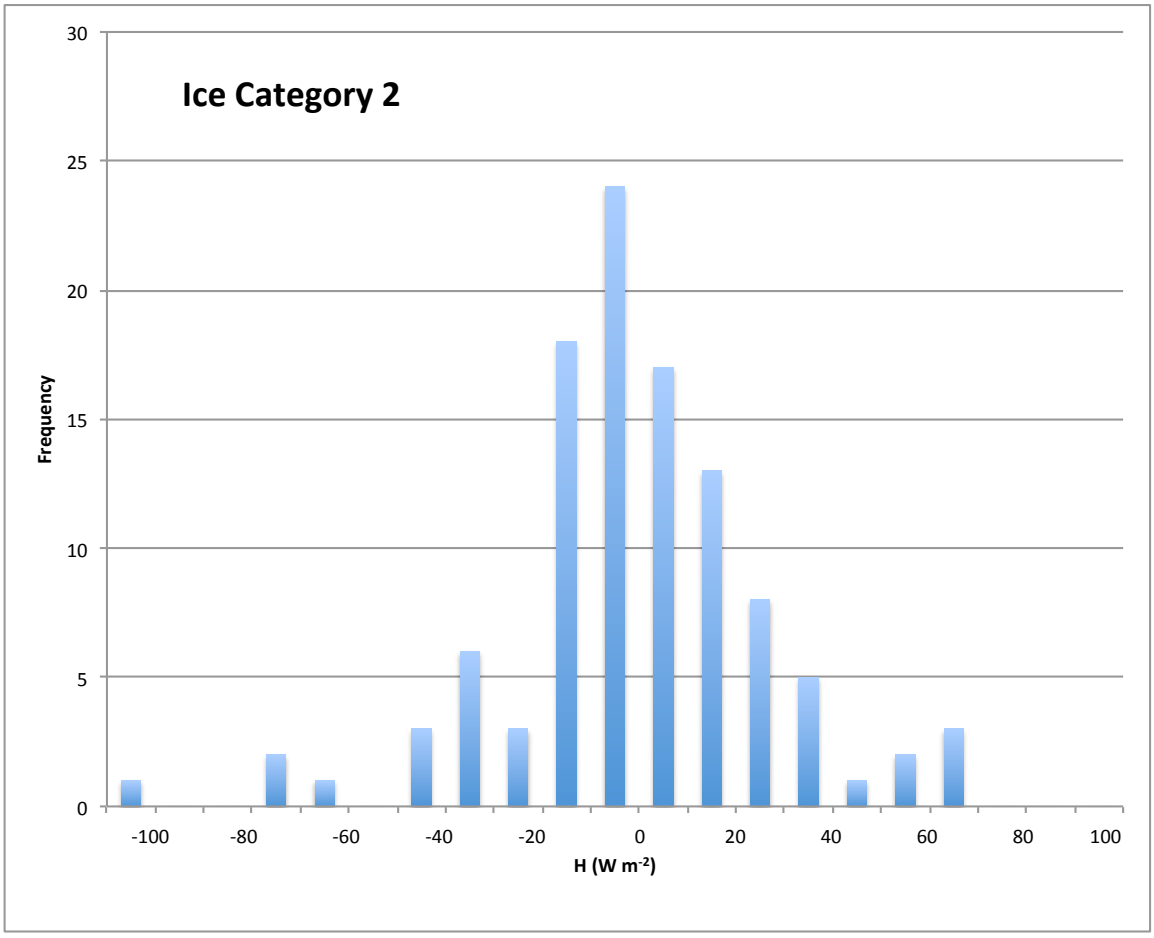

Figure 16. Distribution of sensible heat flux for ice category 2 – in open water.

Ice Category	***1st Quartile***	***Median***	***3rd Quartile***
0	-5.09	0	5.45
1	-4.99	0.24	14.05
2	-11.35	2.13	17.06

Table 3. Quartiles for the three ice category histograms.

Notice the distribution between the three ice categories do not appear to change significantly, although the overall means respond to the coverage of open water.

CHAPTER IV: DISCUSSION

Wintertime regional heat budgets and values estimated for H are not representative for many local scale environments in the Arctic due in large part to the inhomogeneous icescape of varying concentration and thickness. Many studies suggest that H values over the Arctic Ocean average to near 0 W m^{-2} (e.g. Serreze et al., 2007a) yet over smaller spatial and temporal scales actual H values can be quite large. We show that regionally averaged fluxes are indeed small, averaging around -0.016 W m^{-2}, but H values as high as 140 W m^{-2} are not uncommon in lead environments during the winter months.

The temporal evolution of the near surface temperature inversion over sea ice in the Arctic is highly complex, with many different physical processes contributing. These processes include radiative cooling, warm air advection, subsidence, cloud processes, surface melt and topography (Kahl, 1990; Curry, 1983; Busch et al., 1982). Here, we present data that appears to show heating of the lower atmosphere, through the exchange of sensible heat across the ocean-atmosphere interface in open water environments, can modify the evolution of the near surface temperature inversion during the winter.

The observed changes in the temperature structure of the boundary layer could have impacts on diurnal temperatures experienced during the winter months, atmospheric stability (Andreas and Cash, 1999), vertical heat transfer and distribution (Curry et al., 2006), sea ice formation and melt processes (Markus et al., 2009; Maksimovich and Vihma. 2012), cyclone development (Zhang et al., 2004) and even the weather at mid-

latitudes (Francis and Vavrus, 2012). The varying scales of impacts are discussed in subsequent sections.

It is important to keep in mind that it is unlikely that surface heat fluxes are entirely responsible for the temporal evolution of the temperature structure of the lower atmosphere. While the uniquely identified case studies presented here provide an unyielding example of the role that such exchanges can play in the boundary layer, large-scale weather patterns, advections associated with frontal passages and other local effects could have also played a roll in the observed changes in the temperature structure. We expect, however, that mesoscale changes, such as the passage of a cold front, be more represented in the thermal structure over longer temporal scales rather than the smaller scales shown here.

4.1 Implications on the local scale and BL

Warming of the atmospheric column occurred for all periods when positive heat fluxes were measured (ocean to atmosphere flux). Modeling studies have shown that the greatest "flux convergence" or accumulation of heat (warming) occurs in the lowest 20 m of the atmosphere (Curry et al., 1996). With this in mind, the observed effects of enhanced heating on the temperature structure of the boundary layer make physical sense. Inversion strength would be reduced (weaker inversions) because heating would be greater at the lower layers of the atmosphere compared to higher levels, effectively decreasing the temperature difference over the thickness of the inversion. Inversion height would be lowered since the lowest layers of the atmosphere are warmed such that

the region of increasing temperatures with height would occur at lower levels. Finally, inversion depth would increase since warming of the lower levels would mean lower heights and the overall depth over which temperatures increase with height would increase. Raddatz et al., 2010 showed similar results for wintertime inversions in open water environments and indirectly calculated H given information on the temperature and humidty structure of the BL.

Warming in the lower levels would tend to increase instability in the column (Andreas and Cash, 1999) especially during periods of light wind when less vertical mixing occurs. Leads have been shown to drive thermal circulations and lead to the development of convective clouds downwind of open water. (Fett et al., 1997). This can have implications on precipitation (Liu et al, 2012) and radiation budgets (Sedlar et al., 2011; Kay et al., 2008; Wang and Key, 2003; Curry et al., 1996). Increases in precipitation may be more directly related to an enhanced moisture flux due to reduced ice coverage but heat and moisture fluxes are closely connected. A somewhat contrary feedback of local heating leading to more open water and thus more cloud coverage may actually counter some of the large scale heating being observed in the Arctic.

Lowered inversion heights would tend to promote less mixing in the vertical and effectively trap moisture in the lower atmosphere. This could lead to increased moisture near the surface, prolonged fog events and steeper moisture profiles through the boundary layer. This would have implications on large-scale moisture transport, particularly in the development of cyclones. Increased inversion depth would also have similar effects on the temperature and moisture distribution through the BL.

It should be mentioned that the research vessel was influenced by open water for 30 percent of the cases presented. Such environments were similar to those presented in the three unique case studies. These environments were therefore a fairly common occurrence during the course of the study. While these environments are grossly underestimated in today's climate models their spatial coverage is also likely on the rise (Comiso et al., 2008).

While positive fluxes were more common, occasional periods of strong surface heating by the atmosphere (negative fluxes) were also observed. These periods likely had more to do with the synoptic situation than the local micrometeorology. Periods of warm air advection associated with cyclones were noted in this and other studies (eg. Raddatz et al., 2010; Asplin et al., 2012) which would contribute to a warmer atmosphere than was normal. Such exchanges would also be observed more often during the summer months when the atmosphere is quite warm despite the cool water surface (Raddatz et al., 2010).

4.2 Implications on the macroscale

The observations made at the local scale level are also likely to impact the larger scale Arctic and planetary heat budgets. For the Amundsen Gulf region, the wintertime net ocean-atmosphere heat flux depends largely on the extent of open water in the region during the winter months. While older estimates (eg. Barry et al., 1993; Lindsay and Rothrock, 1995) suggest that the open water fraction (leads and polynyas) is on the order of 1 to 5 percent during the winter months, more recent publications suggest an annual

trend in the open water fraction (Else et al., 2011). Open water coverage in the Amundsen Gulf region decreases from 6 percent in November to 1 percent in January (Else et al., 2011). This represents both a more recent and representative estimate of the open water fraction in the Arctic for the winter months. Greater open water coverage leads to both enhanced fluxes and solar heating of the ocean surface (Steele et al., 2008; Perovich et al., 2008). Warming of the lower atmosphere (due to enhanced H fluxes) and the ocean has lead to enhanced ice melt over the past decade (Woodgate et al., 2006). These values and annual trends are likely to continue to change in the coming years (Aagaard and Greisman, 2012).

The fraction of leads, polynyas and open water in general is likely on the rise (Comiso et al., 2008). While the extent of the decline of aerial ice coverage is well documented, few studies have shown an increase in winter leads and polynyas. It is expected that with a weaker, more mobile icescape (Rampal et al., 2009; Spreen et al., 2011; Galley et al., 2013; Kwok et al., 2013) leads and fractures will increase in coverage. An increase in cyclones (discussed below) has also been shown to lead to an increase in the open water fraction (Asplin et al., 2012). An increase in the coverage of such microscale environments would lead to more periods of enhanced heat exchange, significantly altering the heat budget of the Arctic. This further signifies the importance of the measurements presented in this study.

It is important to note that while regionally averaged winter time heat fluxes may be near 0 w m^{-2} (eg. Raddatz et al., 2011; Lindsay, 1998), they may be as high as +140 W m^{-2} over areas of open water. While having implications on the local micrometeorology, these large fluxes are also likely to significantly alter and contribute

to the regional and planetary heat budgets (Ledley, 1988). Studies such as Maykut (1978) and Andreas (1980) suggest that, even at low fractions, these features dominate the regional heat budget for the Arctic Ocean. Regional studies such as the SHEBA experiment found that H varied from -20 to 20 W m^{-2} throughout the course of a year (Persson et al., 2002; Overland et al., 2000). Modeling studies have found similar ranges in values (eg. Tjernstrom et al., 2005). Both regional and modeling studies fail to capture the unique measurements made in local scale environments even though they contribute significantly to the total heat budget. Therefore, it is suggested that many regional and even global heat budget models, which use such values, are underdoing the warming experienced at high latitudes.

If we extrapolate local values from this study to the Amundsen Gulf region (roughly 60,000 km^2) using knowledge of the literature previously highlighted (lead fraction of roughly 6 percent in winter and assuming a flux of 100 W m^{-2}), we can estimate regional heat fluxes to the atmosphere to be 360,000 MJ s^{-1} or 1.296 x 10^9 MWh. If we use the definition of Arctic winter as being DJFM, we get a value of approximately 3.787 x 10^{12} MW of energy transferred into the atmosphere from open water environments during the Arctic winter. Consider the effects of such warming if we applied these values to the entire Arctic Ocean.

While the impacts on the regional and global heat budgets are likely to be significant, a further teleconnection can be made to Arctic cyclones. Studies have shown a significant decreasing trend in sea level pressure over the Arctic Ocean (Serreze et al., 2009; Polyakov et al., 2003) suggesting that cyclones have increased in frequency and intensity in the region (Sepp and Jaagus, 2010). Heat and moisture input from the Ocean

drives cyclone formation, intensification and decay (Asplin et al., 2012; Zhang et al., 2004). An increase in the coverage of leads may help to enhance cyclonic activity (Sepp and Jaagus, 2010). The number of deep Arctic cyclones (having a central pressure less than 1000 hPa) has increased over the last fifty years (Sepp and Jaagus, 2010). While enhanced ocean-atmosphere heat fluxes may be a major contributor to the observed trends in cyclonic behavior, cyclones themselves may be a contributor (Asplin et al., 2012). Cyclones have been shown to cause large-scale fracture events (Asplin at el., 2012), which will further increase the open water coverage and thus the ocean-atmosphere fluxes.

Finally, warming in the lower atmosphere at high latitudes has recently been linked to extreme weather at midlatitudes (Budikova, 2009; Honda et al., 2009; Francis et al., 2009; Overland and Wang, 2010; Petoukhov and Semenov, 2010; Deser et al., 2010; Alexander et al., 2010; Jaiser et al., 2012; Bluthgen et al., 2012; Francis and Vavrus, 2012). The warming of the atmosphere experienced at high latitudes relative to lower latitudes, known as Arctic Amplification (Screen and Simmonds, 2010; Serreze et al., 2009), may cause more persistent weather patterns at mid-latitudes due to a reduced poleward temperature gradient and a resultant weakening of the middle atmospheric winds. A weakening of the jet stream leads to more amplified flow (Mote, 2006; Tedesco et al., 2011), more prolonged weather conditions and a higher likelihood for extreme weather such as droughts and floods (Jaeger and Seneviratne, 2011).

4.3 Future implications

Ongoing and expected changes to the polar seas means that heat fluxes are likely to have further implications. First year or annual sea ice extent is increasing at the expense of multi-year sea ice (Kwok and Cunningham, 2010; Stroeve et al., 2008). First year ice is much more mobile (Hakkinen et al., 2008) and easily deformed by waves and winds which would result in more open water during the winter. With the anomalous heat fluxes measured in open water measurements shown to contribute significantly to the heat budget of the Arctic Ocean, it is expected that a further increase in open water coverage would drastically alter the exchange of heat between the ocean and atmosphere. A second factor is rising global air and sea temperatures but it remains unclear how this would impact the rate of heat exchange between the ocean and atmosphere.

Surface exchanges are the driving force for the world's large-scale climate and weather patterns. Niche measurements such as those presented here, therefore remain critical components of today's global circulation models (GCMs). Current general circulation models have large discrepancies in simulations of the present and predictions of the future climate of the Arctic (e.g., Randall et al. 1998; Knutti, 2008). These difficulties are due, in large part, to an incomplete understanding of the physics of the vertical energy exchanges within the ocean–ice–atmosphere system. The Arctic icescape is also grossly oversimplified in today's climate models with lead and polynya environments often misrepresented or entirely uncaptured. These deficiencies are inherent with GCMs but further exemplify the need for more detailed measurements made on the local scale. Until local scale measurements and processes are incorporated

into the increasingly complex climate models, our understanding and future outlook of the state of the Arctic will remain incomplete.

CHAPTER V: CONCLUSION

Regional estimates of H used in climate models are grossly simplified and underestimated. There is a significant need to account for small-scale processes that occur in ice environments that exist beyond the spatial resolution of many of the world's climate models (Lupkes et al., 2008). The Arctic is a unique physical environment particularly during the winter months when sea ice dominates the surface cover class. The assumption that minimal exchange occurs between the ocean and atmosphere during these months is inaccurate. The highly inhomogeneous nature of the Arctic icescape allows for significant exchanges to occur between the two mediums, particularly in mixed ice-ocean environments such as leads and polynyas. Although small in their spatial coverage, these environments dominate the local and regional heat budgets of the Arctic Ocean. Large fluxes on the order of +140 W m^{-2} were shown by this study to occur in such environments. Some modeling studies have projected that even larger fluxes must occur (eg. Curry et al., 1996). With the ongoing reduction in sea ice extent and thickness, measurements such as those presented here will become increasingly important.

Periods of enhanced surface exchange were shown to modify and contribute to the temporal evolution of the near surface temperature inversion over sea ice during the winter. In particular, periods of enhanced exchange (2.5 times the mean) were shown to be characterized by: 1) lowering of near surface inversions, 2) weakening of near surface inversions, and 3) deepening of near surface inversions. The changing characteristics of the thermal structure of the atmosphere are likely to have impacts on all spatial and

temporal scales, including local and global teleconnections that may impact weather at midlatitudes.

LITERATURE CITED

Alam, A., & Curry, J. A. (1995). Lead-induced atmospheric circulations. *Journal of Geophysical Research*, 100 (C3), 4643-4651.

Alam, A., & Curry, J. A. (1997). Determination of surface turbulent fluxes over leads in Arctic sea ice. *Journal of Geophysical Research*, 102 (C2), 3331-3343.

Alam, A., & Curry, J. A. (1998). Evolution of new ice and turbulent fluxes over freezing winter leads. *Journal of Geophysical Research*, 103 (C8), 15783-15802.

Anctil, F., Donelan, M.A., Drennan, W.M. Eddy-correlation measurements of air-sea fluxes from a discus buoy. *Journal of Atmospheric and Oceanic technology*, 11.4, 1144-1150.

Anderson, P. S., & Neff, W. D. (2008). Boundary layer physics over snow and ice. *Atmospheric Chemistry and Physics*, 8, 3563–3582.

Andreas E.L. (2002) Parameterizing scalar transfer over snow and ice: a review. *J of Hydrometeorology* 3:417-432.

Andreas E.L., Horst T.W., Grachev A.A., Persson P.O.G, Fairall C.W., Guest P.S., Jordan R.E. (2010b). Parameterizing turbulent exchange over summer sea ice and the marginal ice zone. *QJR. Meteorol Soc* 136:927–943.

Andreas E.L., Persson P.O.G., Jordan R.E., Horst T.W., Guest P.S., Grachev A.A., Fairall C.W. (2010a). Parameterizing turbulent exchange over sea ice in winter. *J Hydrometeorology* 11:87-104.

Andreas, E. L. (1980). Estimation of heat and mass fluxes over Arctic leads. *Monthly Weather Review*, *108*(12), 2057-2063.

Andreas, E. L., & Cash, B. A. (1999). Convective heat transfer over wintertime leads and polynyas. *Journal of Geophysical Research: Oceans (1978–2012)*,*104*(C11), 25721-25734.

Andreas, E. L., & Cash, B. A. (1999). Convective heat transfer over wintertime leads and polynyas. Journal of Geophysical Research, 104, 25721–25734.

Andreas, E. L., Paulson, C. A., Williams, R. M., Lindsay, R. W., & Businger, J. A. (1979). The turbulent heat flux from Arctic leads. *Boundary Layer Meteorology*, 17, 57-91.

Arya, P. S. (2001). Introduction to Micrometeorology, 2nd edn. Academic Press, San Diego, CA, 420 pp

Asplin, M. G., Galley, R., Barber, D. G., & Prinsenberg, S. (2012). Fracture of summer perennial sea ice by ocean swell as a result of Arctic storms. *Journal of Geophysical Research: Oceans (1978–2012)*, *117*(C6).
Baldocchi, D. D. (2003). Assessing the eddy covariance technique for evaluating carbon dioxide exchange rates of ecosystems: past, present and future. *Global Change Biology*, *9*(4), 479-492.

Barber, D. G., Asplin, M. G., Gratton, Y., Lukovich, J. V., Galley, R. J.,Raddatz, R. L., & Leitch, D. (2010). The International Polar Year (IPY) Circumpolar Flaw Lead (CFL) system study: Overview and the physical system. *Atmosphere-Ocean*, 48, 225–243.

Barry, R. G. (1983). Arctic Ocean ice and climate: Perspectives on a century of polar research. *Annals of the Association of American Geographers*, *73*(4), 485-501.

Barry, R. G., Serreze, M. C., Maslanik, J. A., & Preller, R. H. (1993). The Arctic sea ice climate system: observations and modeling. *Review of Geophysics*, 31 (4), 397-422.

Blanc, T. V. (1985). Variation of bulk-derived surface flux, stability, and roughness results due to the use of different transfer coefficient schemes. *Journal of physical oceanography*, 15(6), 650-669.

Blüthgen, J., Gerdes, R., & Werner, M. (2012). Atmospheric response to the extreme Arctic sea ice conditions in 2007. *Geophysical Research Letters*, *39*(2).

Bradley, R. S., Keimig, F. T., & Diaz, H. F. (1992). Climatology of surface-based inversions in the North American Arctic. *Journal of Geophysical Research: Atmospheres (1984–2012)*, *97*(D14), 15699-15712.

Brown R, Bartlett P, MacKay M, Verseghy D (2006) Evaluation of snow cover in CLASS for SnowMIP. Atmosphere-Ocean 44:223-238.

Budikova, D. (2009). Role of Arctic sea ice in global atmospheric circulation: A review. *Global and Planetary Change*, *68*(3), 149-163.

Burba, G. G., McDermitt, D. K., Grelle, A., Anderson, D. J., & Xu, L. (2008). Addressing the influence of instrument surface heat exchange on the measurements of CO2 flux from open□path gas analyzers. *Global Change Biology*, *14*(8), 1854-1876.

Busch, D. M. N., Ebel, D. M. U., Kraus, H., & Schaller, E. (1982). The structure of the subpolar inversion-capped ABL. *Archives for meteorology, geophysics, and bioclimatology, Series A*, *31*(1-2), 1-18.

Candlish, L. M., Raddatz, R. L., Asplin, M. G., & Barber, D. G. (2012). Atmospheric temperature and absolute humidity profiles over the Beaufort Sea and Amundsen Gulf from a microwave radiometer. *Journal of Atmospheric and Oceanic Technology*, *29*(9), 1182-1201.
Chou, S.H. (1993). A comparison of airborne eddy correlation and bulk aerodynamic methods for ocean-air turbulent fluxes during cold-air outbreaks. *Boundary-Layer Meteorology*. Issue 64, Pages 75-100.

Collins W.D., Bitz C.M., Blackmon M.L., Bonan G.B., Bretherton C.S., Carton J.A., Chang P., Doney S.C., Hack J.J., Henderson T.B., Kiehl J.T., Large W.G., McKenna D.S., Santer B.D., Smith R.D. (2006). The Community Climate System Model version 3 (CCSM3). *J Climate* 19:2122–2143.

Comiso, J. C., Parkinson, C. L., Gersten, R., & Stock, L. (2008). Accelerated decline in the Arctic sea ice cover. *Geophysical Research Letters*, 35 (1).

Curry, J. (1983). On the formation of continental polar air. *Journal of the Atmospheric Sciences*, 40(9), 2278-2292.

Curry, J. A., Schramm, J. L., Rossow, W. B., & Randall, D. (1996). Overview of Arctic cloud and radiation characteristics. *Journal of Climate*, *9*(8), 1731-1764.

Deser, C., Tomas, R., Alexander, M., & Lawrence, D. (2010). The seasonal atmospheric response to projected Arctic sea ice loss in the late twenty-first century. *Journal of Climate*, *23*(2), 333-351.

Drue, C., & Heinemann, G. (2007). Characteristics of intermittent turbulence in the upper stable boundary layer over Greenland. *Boundary Layer Meteorology*, 124, 361–381.

Dyer, J. L., & Mote, T. L. (2006). Spatial variability and trends in observed snow depth over North America. *Geophysical Research Letters*, *33*(16).

Else, B. G. T., Papakyriakou, T. N., Galley, R. J., Drennan, W. M., Miller, L. A., & Thomas, H. (2011). Wintertime CO2 fluxes in an Arctic polynya using eddy covariance: Evidence for enhanced air□sea gas transfer during ice formation. *Journal of Geophysical Research: Oceans (1978–2012)*, 116(C9).

Fett, R. W., Englebretson, R. E., & Burk, S. D. (1997). Techniques for analyzing lead condition in visible, infrared and microwave satellite imagery. *Journal of Geophysical Research: Atmospheres (1984–2012)*, *102*(D12), 13657-13671.

Francis, J. A., & Vavrus, S. J. (2012). Evidence linking Arctic amplification to extreme weather in mid□latitudes. *Geophysical Research Letters*, 39(6).

Francis, J. A., Chan, W., Leathers, D. J., Miller, J. R., & Veron, D. E. (2009). Winter Northern Hemisphere weather patterns remember summer Arctic sea□ice extent. *Geophysical Research Letters*, *36*(7).

Friehe, C. A., & Schmitt, K. F. (1976). Parameterization of air-sea interface fluxes of sensible heat and moisture by the bulk aerodynamic formulas. *Journal of Physical Oceanography*, *6*(6), 801-809.

Galley, R. J., Else, B. G., Howell, S. E., Lukovich, J. V., & Barber, D. G. (2012). Landfast sea ice conditions in the Canadian Arctic: 1983-2009. *Arctic*, 133-144.

Galley, R. J., Key, E., Barber, D. G., Hwang, B. J., & Ehn, J. (2008). Spatial and temporal variability of sea ice in the southern Beaufort Sea and Amundsen Gulf: 1980–2004. *Journal of Geophysical Research*, 113, C05S95.

Goulden, M. L., Munger, J. W., FAN, S. M., Daube, B. C., & Wofsy, S. C. (1996). Measurements of carbon sequestration by long□term eddy covariance: Methods and a critical evaluation of accuracy. *Global change biology*, *2*(3), 169-182.

Grachev, A. A., & Panin, G. N. (1984). Parameterization of the sensible and latent heat fluxes above the water surface in calm weather under natural conditions. *Izv. Atmos. Oceanic Phys*., 20, 371-376.

Gultepe, I., Isaac, G. A., Williams, A., Marcotte, D., Strawbridge, K.B. (2003). Turbulent heat fluxes over leads and polynyas, and their effects on Arctic clouds during FIRE.ACE: Aircraft observations for April, 1988. *Atmosphere-Ocean*, 41, 15-34.

Hakkinen, S., Proshutinsky, A., & Ashik, I. (2008). Sea ice drift in the Arctic since the 1950s. *Geophysical Research Letters*, *35*(19).

Higgins, M. E., & Cassano, J. J. (2009). Impacts of reduced sea ice on winter Arctic atmospheric circulation, precipitation, and temperature. *Journal of Geophysical Research: Atmospheres (1984–2012)*, *114*(D16).

Honda, M., Inoue, J., & Yamane, S. (2009). Influence of low Arctic sea□ice minima on anomalously cold Eurasian winters. *Geophysical Research Letters*, *36*(8).

Horst, T.W. (2003). Attenuation of scalar fluxes measured with displaced sensors. EGS-AGU-EUG Joint Assembly, April 6-11, 2003, Nice, France.

Jaeger, E. B., & Seneviratne, S. I. (2011). Impact of soil moisture–atmosphere coupling on European climate extremes and trends in a regional climate model. *Climate Dynamics*, *36*(9-10), 1919-1939.

Jaiser, R., Dethloff, K., Handorf, D., Rinke, A., & Cohen, J. (2012). Impact of sea ice cover changes on the Northern Hemisphere atmospheric winter circulation. *Tellus A*, *64*.

Järvi, L., Mammarella, I., Eugster, W., Ibrom, A., Siivola, E., Dellwik, E., Vesala, T. (2009). Comparison of net CO2 fluxes measured with open-and closed-path infrared gas analyzers in an urban complex environment. *Boreal Environment Research*, *14*, 499-514.
Kahl, J. D. (1990). Characteristics of the low□level temperature inversion along the Alaskan Arctic coast. *International journal of climatology*, *10*(5), 537-548.

Kinnard, C., Zdanowicz, C. M., Fisher, D. A., Isaksson, E., Vernal, A., & Thompson, L. G. (2011). Reconstructed changes in Arctic sea ice over the past 1,450 years. *Nature*, 479, 509-513.
Knutti R. 2008. Should we believe model predictions of future climate change? *Phil. Trans. R. Soc.* 366: 4647–4664.

Kondo, J. (1975). Air-sea bulk transfer coefficients in diabatic conditions. *Boundary-Layer Meteorology*, *9*(1), 91-112.

Kottmeier, C., & Engelbart, D. (1991). Generation and atmospheric heat exchange of coastal polynyas in the Weddell Sea. *Boundary Layer Meteorology*, 60, 207-234.

Kurtz, N. T., Markus, T., Farrell, S. L., Worthen, D. L., & Boisvert, L. N. (2011). Observations of recent Arctic sea ice volume loss and its impact on ocean-atmosphere energy exchange and ice production. *Journal of Geophysical Research* , 116 (C04015), 1-19.

Kwok, R. (2007). Near zero replenishment of the Arctic multiyear sea ice cover at the end of 2005 summer. *Geophysical Research Letters*, 34 (5), 1-6.

Kwok, R., & Cunningham, G. F. (2010). Contribution of melt in the Beaufort Sea to the decline in Arctic multiyear sea ice coverage: 1993-2009. *Geophysical Research Letters*, 37, 1-5.

Kwok, R., Spreen, G., & Pang, S. (2013). Arctic sea ice circulation and drift speed: Decadal trends and ocean currents. *Journal of Geophysical Research: Oceans*, *118*(5), 2408-2425.

Laikhtman, D.L., Klyuchnikova, L.A. (1957). The role of fractures in the heat balance of the Arctic. *Tr. Gl. Geofiz. Obs. im. AI Voeikova*, *69*, 77-79.

Ledley, T. S. (1988). A coupled energy balance climate-sea ice model: impact of sea ice and leads on climate. *Journal of Geophysical Research*, 95 (15), 919-932.

Lindsay, R. W. (1998). Temporal variability of the energy balance of thick Arctic pack ice. *Journal of Climate*, *11*(3), 313-333.

Lindsay, R. W., & Rothrock, D. A. (1995). Arctic sea ice leads from advanced very high resolution radiometer images. *Journal of Geophysical Research: Oceans (1978–2012)*, *100*(C3), 4533-4544.

Liu, J., Curry, J. A., Wang, H., Song, M., & Horton, R. M. (2012). Impact of declining Arctic sea ice on winter snowfall. *Proceedings of the National Academy of Sciences*, *109*(11), 4074-4079.
Lupkes, C., Vihma, T., Birnbaum, G., Wacker, U. (2008). Influence of leads in sea ice on the temperature of the atmospheric boundary layer during polar night. *Geophysical Research Letters*, 35.

Maksimovich E., Vihma T. (2012). The effect of surface heat fluxes on interannual variability in the spring onset of snow melt in the central Arctic Ocean. *J Geophysic Res* 117:C07012.

Manabe, S., & Stouffer, R. J. (1980). Sensitivity of a global climate model to an increase of CO2 in the atmosphere. *Journal of Geophysical Research*, 85, 5529-5554.

Marcq, S., & Weiss, J. (2011). Influence of leads widths distribution of turbulent heat transfer between the ocean and the atmosphere. *The Cryosphere Discussions* , 5, 2765-2797.

Markus T, Stroeve JC, Miller J (2009) Recent changes in Arctic sea ice melt onset, freezeup, and melt season length. *J Geophysic Res* 114:C12024.

Maslanik, J., Stroeve, J., Fowler, C., & Emery, W. (2011). Distribution and trends in Arctic sea ice age through spring 2011. *Geophysical Research Letters*, 38, 1-6.

Massman, W. J. (2000). A simple method for estimating frequency response corrections for eddy covariance systems. *Agricultural and Forest Meteorology*,*104*(3), 185-198.

Maykut, G. A. (1978). Energy exchange over young sea ice in the Central Arctic. *Journal of Geophysical Research*, 83 (C7), 3646-3658.

Maykut, G. A. (1982). Large-scale heat exchange and ice production in the Central Arctic. *Journal of Geophysical Research*, 87 (C10), 7971-7984.

Mitsuta, Y., & Fujitani, T. (1974). Direct measurement of turbulent fluxes on a cruising ship. *Boundary-Layer Meteorology*, *6*(1-2), 203-217.

Nakamura, N., & Oort, A. H. (1988). Atmospheric heat budgets of the polar regions. *Journal of Geophysical Research: Atmospheres (1984–2012)*, *93*(D8), 9510-9524.

Oke, T. R. (1987). Boundary layer climates, 2nd edn. Methuen, London, 435 pp

Overland, J. E. (2009). Meteorology of the Beaufort Sea. *Journal of Geophysical Research: Oceans (1978–2012)*, *114*(C1).

Overland, J. E., & Guest, P. S. (1991). The Arctic snow and air temperature budget over sea ice during winter. *Journal of Geophysical Research: Oceans (1978–2012)*, *96*(C3), 4651-4662.

Overland, J. E., & Wang, M. (2005). The Arctic climate paradox: The recent decrease of the Arctic Oscillation. *Geophysical Research Letters*, *32*(6).

Overland, J. E., & Wang, M. (2010). Large□scale atmospheric circulation changes are associated with the recent loss of Arctic sea ice. *Tellus A*, *62*(1), 1-9.

Overland, J. E., McNutt, S. L., Groves, J., Salo, S., Andreas, E. L., & Persson, P. (2000). Regional sensible and radiative heat flux estimates for the winter Arctic during the Surface Heat Budget of the Arctic Ocean (SHEBA) experiment. *Journal of Geophysical Research*, 105 (C6), 14093-14102.

Parkinson, C., Cavalieri, D., Gloersen, P., Zwally, H., & Comiso, J. (1999). Arctic sea ice extents, areas, and trends, 1978–1996. *Journal of Geophysical Research, 104*(C9), 20837-20856.

Pavelsky, T. M., Boé, J., Hall, A., & Fetzer, E. J. (2011). Atmospheric inversion strength over polar oceans in winter regulated by sea ice. *Climate Dynamics*, *36*(5-6), 945-955.

Penner, C. M. (1955). A three-front model for synoptic analyses. *Quarterly Journal of the Royal Meteorological Society*, 81, 89–91.

Perovich, D. K., Richter□Menge, J. A., Jones, K. F., & Light, B. (2008). Sunlight, water, and ice: Extreme Arctic sea ice melt during the summer of 2007. *Geophysical Research Letters*, *35*(11).

Persson, O. P. G., Fairall, C. W., Andreas, E. L., Guest, P. S., & Perovich, D.K. (2002). Measurements near the atmospheric surface flux group tower at SHEBA: Near-surface conditions and surface energy budget. *Journal of Geophysical Research*, 107(C10), 8045.

Petoukhov, V., & Semenov, V. A. (2010). A link between reduced Barents□Kara sea ice and cold winter extremes over northern continents. *Journal of Geophysical Research: Atmospheres (1984–2012)*, *115*(D21).

Pielke, R., Avissar, R., Raupach, M., Dolman, J., Zeng, X., & Denning, S. (1998). Interactions between the atmosphere and terrestrial ecosystems: Influence on weather and climate. *Global Change Biology,* 461-475.

Pinto, J. O., Alam, A., Maslanik, J. A., Curry, J. A., Stone, R. S. (2003). Surface chracteristics and atmospheric footprint of springtime Arctic leads at SHEBA. *Journal of Geophysical Research*, 108(C4).

Polyakov, I. V., Bekryaev, R. V., Alekseev, G. V., Bhatt, U. S., Colony, R. L., Johnson, M. A., Walsh, D. (2003). Variability and trends of air temperature and pressure in the maritime Arctic, 1875-2000. *Journal of Climate*, *16*(12), 2067-2077.

Raddatz RL, Galley RJ, Candlish LM, Asplin MG and Barber DG. (2013). Integral profile estimates of sensible heat flux from an unconsolidated sea-ice surface. *Atmosphere-Ocean,* 51(2), 135-144

Raddatz, R. L., Asplin, M. G., Candlish, L., Barber, D.G. (2011). General characteristics of the atmospheric boundary layer over a flaw lead polynya region for winter and spring. *Boundary-Layer Meteorology*.

Raddatz, R. L., Galley, R.J., Barber, D.G. (2012). Linking the atmospheric boundary layer to the Amundsen Gulf sea-ice cover: A mesoscale to synoptic-scale perspective from winter to summer 2008. *Boundary-Layer Meteorology*.

Rampal, P., Weiss, J., & Marsan, D. (2009). Positive trend in the mean speed and deformation rate of Arctic sea ice, 1979–2007. *Journal of Geophysical Research: Oceans (1978–2012)*, *114*(C5).

Randall, D., Curry, J., Battisti, D., Flato, G., Grumbine, R., Hakkinen, D.,Weatherly, J. (1998). Status and outlook for large scale modeling of atmosphere-ice-ocean interactions in the Arctic. *Bulletin of the American Meteorological Society*, 79, 197–219.

Rothrock, D. A., Yu, Y., & Maykut, G. A. (1999). Thinning of the Arctic Sea-Ice Cover. *Geophysical Research Letters*, 26 (23), 3469-3472.

Schotanus, P. Nieuwstadt, F.T.M. DeBruin, H.A.R. (1983). Temperature measurement with a sonic anemometer and its application to heat and moisture fluctuations. *Boundary-Layer Meteorology*. Volume 26, Pages 81-93.

Screen, J. A., & Simmonds, I. (2010). The central role of diminishing sea ice in recent Arctic temperature amplification. *Nature*, *464*(7293), 1334-1337.

Sedlar J., Tjernstrom M., Mauritsen T., Shupe. M.D., Brooks I.M., Persson P.O.G., Birch C.E., Leck C., Sirevaag A., Nicolaus M. (2011) A transitioning Arctic surface energy budget: the impacts of solar zenith angle, surface albedo and cloud radiative forcing. *Clim Dyn* 37:1643–1660.

Sepp, M., & Jaagus, J. (2011). Changes in the activity and tracks of Arctic cyclones. *Climatic Change*, *105*(3-4), 577-595.

Serreze, M. C., & Barry, R. G. (2005). *The Arctic climate system* (Vol. 22). Cambridge University Press.

Serreze, M. C., Barrett, A. P., Slater, A. G., Steele, M., Zhang, J., & Trenberth, K. E. (2007). The large-scale energy budget of the Arctic. *Journal of Geophysical Research*, 112, D11122.

Serreze, M. C., Barrett, A. P., Stroeve, J. C., Kindig, D. N., & Holland, M. M. (2009). The emergence of surface-based Arctic amplification. *The Cryosphere*, *3*(1), 11-19.
Serreze, M. C., Box, J. E., Barry, R. G., & Walsh, J. E. (1993). Characteristics of Arctic synoptic activity, 1952–1989. *Meteorology and Atmospheric Physics*, *51*(3-4), 147-164.

Serreze, M. C., Holland, M. M., & Stroeve, J. (2007). Persepctives on the Arctic's shrinking sea-ice cover. *Science*, 315 (1533), 1533-1536.

Serreze, M. C., Schnell, R. C., & Kahl, J. D. (1992). Low-level temperature inversions of the Eurasian Arctic and comparisons with Soviet drifting station data. *Journal of Climate*, *5*(6), 615-629.

Serreze, M., Maslanik, J., & Scambos, T. (2003). A record minimum arctic sea ice extent and area in 2002. *Geophysical Research Letters,* 3*0*(3).

Simmonds, I., & Keay, K. (2009). Extraordinary September Arctic sea ice reductions and their relationships with storm behavior over 1979–2008. *Geophysical Research Letters*, *36*(19).

Simmonds, I., & Rudeva, I. (2012). The great Arctic cyclone of August 2012. *Geophysical research letters*, *39*(23).

Sirevaag, A., Rosa, S. D. L., Fer, I., Nicolaus, M., Tjernström, M., & McPhee, M. G. (2011). Mixing, heat fluxes and heat content evolution of the Arctic Ocean mixed layer. *Ocean Science Discussions*, *8*(1), 247-289.

Smith, S., Muench, R. D., & Pease, C. (1990). Polynyas and leads: an overview of physical processes and environment. *Journal of Geophysical Research*, 95, 9461-9479.

Spreen, G., Kwok, R., & Menemenlis, D. (2011). Trends in Arctic sea ice drift and role of wind forcing: 1992–2009. *Geophysical Research Letters*, *38*(19).

Steele, M., Ermold, W., & Zhang, J. (2008). Arctic Ocean surface warming trends over the past 100 years. *Geophysical Research Letters*, *35*(2).

Stroeve, J. Serreze, J.C. Fetterer, F. (2005). Tracking the Arctic's shrinking ice cover: Another extreme September minimum in 2004. *Geophysical Research Letters*, 32(4).

Stroeve, J., Serreze, M., Drobot, S., Gearheard, S., Holland, M., Maslanik, J. (2008). Arctic sea ice extent plummets in 2007. *EOS Transactions American Geophysical Union*, 89 (2), 13-14.

Stull, R.B. (1988). An Introduction to Boundary Layer Meteorology. Kluwer Academic Publishers, Dordrecht, The Netherlands, 670 pp.

Tedesco, M., Fettweis, X., Van den Broeke, M. R., Van de Wal, R. S. W., Smeets, C. J. P. P., van de Berg, W. J., ... & Box, J. E. (2011). The role of albedo and accumulation in the 2010 melting record in Greenland.*Environmental Research Letters*, *6*(1), 014005.

Tjernström, M., Žagar, M., Svensson, G., Cassano, J. J., Pfeifer, S., Rinke, A., Shaw, M. (2005). Modelling the Arctic boundary layer: an evaluation of six ARCMIP regional-scale models using data from the SHEBA project. *Boundary-Layer Meteorology*, *117*(2), 337-381.

Twine, T. E., Kustas, W. P., Norman, J. M., Cook, D. R., Houser, P., Meyers, T. P., Wesely, M. L. (2000). Correcting eddy-covariance flux underestimates over a grassland. *Agricultural and Forest Meteorology*, *103*(3), 279-300.

Wadhams, P., & Davis, N. R. (2000). Further evidence of ice thinning in the Arctic Ocean. *Geophysical Research Letters*, *27*(24), 3973-3975.

Wang, X., & Key, J. R. (2003). Recent trends in Arctic surface, cloud, and radiation properties from space. *Science*, *299*(5613), 1725-1728.

Webb, E. K., Pearman, G. I., & Leuning, R. (1980). Correction of flux measurements for density effects due to heat and water vapour transfer. *Quarterly Journal of the Royal Meteorological Society*, *106*(447), 85-100.

Webb, E.K. Pearman, G.I. Leuning, R. (1980). Correction of flux measurements for density effects due to heat and water vapor transfer. *Quart. J. Roy. Meteorol. Soc*. Volume 106, Pages 85-100.

Woodgate, R. A., Aagaard, K., & Weingartner, T. J. (2006). Interannual changes in the Bering Strait fluxes of volume, heat and freshwater between 1991 and 2004. *Geophysical Research Letters*, *33*(15).

Zhang, X., Ikeda, M., & Walsh, J. E. (2003). Arctic sea ice and freshwater changes driven by the atmospheric leading mode in a coupled sea ice-ocean model. *Journal of Climate*, *16*(13), 2159-2177.

Zhang, X., Walsh, J. E., Zhang, J., Bhatt, U. S., & Ikeda, M. (2004). Climatology and interannual variability of Arctic cyclone activity: 1948-2002. *Journal of Climate*, *17*(12), 2300-2317.